Theory of Inversion of Dispersive Bi-Isotropic Slab Parameters using TEM-Pulses

Rikte, Sten

1997

CODEN:LUTEDX/(TEAT-7055)/1-29/(1997)

Theory of Inversion of Dispersive Bi-Isotropic Slab Parameters using TEM-Pulses

Sten Rikte

Department of Electroscience
Electromagnetic Theory
Lund Institute of Technology
Sweden

Sten Rikte

Department of Electromagnetic Theory
Lund Institute of Technology
P.O. Box 118
SE-221 00 Lund
Sweden

Editor: Gerhard Kristensson

Abstract

A new method of reconstructing the causal susceptibility kernels of a homogeneous, temporally dispersive, bi-isotropic medium from generic scattering data at normal incidence is presented. This inverse problem is shown to be well posed in the space of continuous functions furnished with the maximum norm, $C[0,T]$. A numerical example is given.

1 Introduction

Natural bi-isotropic materials (isotropic chiral media or optically active media) are known at least since the days of Napoleon [1, 2, 5]. These substances interact with light. The first experiments involving man-made chiral materials and Hertzian waves were performed by Lindman in the beginning of this century [13]. During the past decade, considerable attention has been paid to the interaction between microwaves and artificial bi-isotropic media [4, 11]. This interest is due to the potential use for these materials in various electronic devices. Bi-isotropic materials are of importance within the fields of biology and chemistry as well. For basic, time-harmonic, electromagnetic theory and applications for bi-isotropic materials, and for further references, the reader is referred to the book by Lindell *et al.* [12].

Bi-isotropic materials are "handed" on a microscopic scale. The general bi-isotropic medium is characterized by four (real-valued) time-dependent susceptibility functions: the electric susceptibility kernel, the magnetic susceptibility kernel, the chirality kernel, and the non-reciprocity kernel. The electric and magnetic susceptibility kernels are the convolution kernels of the permittivity and the permeability operators of the medium, respectively. The chirality kernel and the non-reciprocity kernel represent the constitutive coupling between the electric and the magnetic field quantities that is typical for bi-isotropic materials.

The most salient feature of the isotropic chiral medium is perhaps the optical rotatory power (ORP): the plane of polarization of a monochromatic, linearly polarized (LP) plane wave rotates as the wave propagates through the medium. This phenomenon can be explained by the fact that each LP plane wave can be written as the sum of one right-circularly polarized (RCP) plane wave and one left-circularly polarized (LCP) plane wave with identical amplitudes, and that these (eigen-) waves travel through the medium with different phase speeds. This applies to idealized non-absorbing materials for which the phase speeds are real. Monochromatic wave propagation in absorbing isotropic chiral materials exhibits a distortion of polarization as well (elliptical polarization). This phenomenon is referred to as circular dichroism (CD). In absorbing isotropic chiral materials, the phase speeds are complex-valued with different real and imaginary parts.

Pulse propagation in material media is complicated by temporal dispersion. In bi-isotropic materials, material dispersion gives rise to so called optical rotatory dispersion: each excited elementary RCP plane wave or LCP plane wave propagates with a complex-valued phase speed that depends on the frequency. The four time-dependent susceptibility kernels referred to above model these dispersive ef-

fects properly. Although models for the susceptibility kernels of the bi-isotropic medium have been proposed, e.g., Lorentz' model for the electric susceptibility kernel and Condon's model for the chirality kernel, these functions are, in general, unknown [12]. This is, of course, unsatisfactory in the applications. As a matter of fact, the physics of bi-isotropic materials is not yet properly understood.

One way to gain further insight in the structure of a bi-isotropic material is to apply an inverse algorithm to experimental scattering data. In the early 1990's, several inverse methods were developed using transverse electric and magnetic (TEM) scattering data from bi-isotropic slabs. A frequency-domain method for inversion of isotropic chiral material parameters was suggested by Cloete and Smith [3]. This inverse method requires knowledge of the reflection and transmission coefficients as functions of frequency. Kristensson and Rikte proposed a time-domain method based on the wave-splitting technique [9, 15]. In this method, finite time-traces of the (co- and cross-) reflected and transmitted electric fields are assumed to be known. In the present paper, the time-domain technique is in focus.

Several cases of successful reconstructions with synthetic scattering data were reported in Ref. 15. Single-resonance and double-resonance models (Lorentz' and Condon's models) and relaxation models (Debye's model) were used for the generation of scattering data. In the applied inverse algorithm, the (co- and cross-) reflection and transmission kernels, which are the classical contributions to the impulse response of the slab, and therefore can be considered as the generic quantities of the medium, constitute data. The reflection and transmission kernels are obtained from the reflected and transmitted fields by deconvolution. To avoid the so called inverse crime, the imbedding method was used at the generation of scattering data, whereas the Green functions method was employed in the inversion of the susceptibility kernels. Unfortunately, experimental transient scattering data from bi-isotropic materials was not available.

Issues concerning unique solubility and continuous dependence on generic scattering data were not addressed in Refs [9, 15]. Since deconvolution is an ill-posed problem, these questions are not only of theoretical interest.

The present article is the last in a series of two articles concerning transient direct and inverse scattering from bi-isotropic slabs. The aim with these articles is to summarize previous results and to improve the theory of especially the inverse scattering problem. In the first article, the propagation of electromagnetic pulses in the general bi-isotropic medium is addressed, and a scattering relation in terms of wave propagators and single-interface scattering operators is presented [16]. These quantities are temporal integral operators, whose dependence on the susceptibility kernels of the medium is given explicitly. The corresponding inverse scattering problem is discussed in this second article.

In Section 2, results from Ref. 16, which are relevant for the inverse problem, are recapitulated. In Section 3, it is shown, that, the generic inverse scattering problem for the homogeneous, optically impedance-matched, temporally dispersive bi-isotropic slab is well posed in the space of continuous functions furnished with the maximum norm, $C[0, T]$. As a by-product, a new inverse method is presented. A numerical example using the new technique is given as well. Finally, the scattering

problem for the optically impedance-mismatched slab is analyzed in an appendix.

2 The propagation problem

In this section, appropriate concepts for solving the TEM scattering problem for the bi-isotropic slab are introduced. Throughout the section, the emphasis is on the propagation of time-varying electromagnetic waves in a bi-isotropic medium, whose dispersive properties are known. The inverse problem is discussed in Section 3. For a thorough explanation of the introduced concepts, the reader is referred to Ref. 16.

2.1 Basic equations

Throughout this article, rectangular coordinates $O(x, y, z)$ are employed. The radius vector is written $\boldsymbol{r} = \boldsymbol{e}_x x + \boldsymbol{e}_y y + \boldsymbol{e}_z z$, where $\boldsymbol{e}_x$, $\boldsymbol{e}_y$, and $\boldsymbol{e}_z$ are the basis vectors in the x-, y-, and z-directions, respectively. Time is denoted by t.

The electric and magnetic field intensities at $(\boldsymbol{r}, t)$ are denoted by $\boldsymbol{E}(\boldsymbol{r}, t)$ and $\boldsymbol{H}(\boldsymbol{r}, t)$, respectively, and the corresponding flux densities are $\boldsymbol{D}(\boldsymbol{r}, t)$ and $\boldsymbol{B}(\boldsymbol{r}, t)$. Each field vector is written in the form

$$\boldsymbol{E} = \boldsymbol{u}_x E_x(\boldsymbol{r}, t) + \boldsymbol{u}_y E_y(\boldsymbol{r}, t) + \boldsymbol{u}_z E_z(\boldsymbol{r}, t).$$

The speed of light in vacuum is c and the intrinsic impedance of vacuum η.

The constitutive relations of a linear, causal, time-invariant, and homogeneous bi-isotropic medium are

$$\begin{aligned} c\eta \boldsymbol{D}(\boldsymbol{r}, t) &= \boldsymbol{E}(\boldsymbol{r}, t) + (\chi_{ee} * \boldsymbol{E})(\boldsymbol{r}, t) + \eta(\chi_{em} * \boldsymbol{H})(\boldsymbol{r}, t), \\ c\boldsymbol{B}(\boldsymbol{r}, t) &= (\chi_{me} * \boldsymbol{E})(\boldsymbol{r}, t) + \eta \boldsymbol{H}(\boldsymbol{r}, t) + \eta(\chi_{mm} * \boldsymbol{H})(\boldsymbol{r}, t), \end{aligned} \tag{2.1}$$

where temporal convolution is denoted by a star:

$$(\chi_{ee} * \boldsymbol{E})(\boldsymbol{r}, t) = \int_{-\infty}^{t} \chi_{ee}(t - t') \boldsymbol{E}(\boldsymbol{r}, t')\, dt'.$$

These constitutive relations are physically sound [7]. The susceptibility kernels vanish for $t < 0$ due to causality and are assumed to be bounded and continuously differentiable for $t > 0$. In this article, the electric susceptibility kernel, $\chi_{ee}(t)$, is written as the sum and the magnetic susceptibility kernel, $\chi_{mm}(t)$, as the difference of two integral kernels, $G(t)$ and $F(t)$:

$$\chi_{ee}(t) = G(t) + F(t), \qquad \chi_{mm}(t) = G(t) - F(t).$$

The cross-coupling susceptibility kernels, $\chi_{em}(t)$ and $\chi_{me}(t)$, are written as a sum and a difference as well:

$$\chi_{em}(t) = K(t) + L(t), \qquad \chi_{me}(t) = -K(t) + L(t),$$

where the functions $K(t)$ and $L(t)$ are the chirality and the non-reciprocity kernels, respectively.

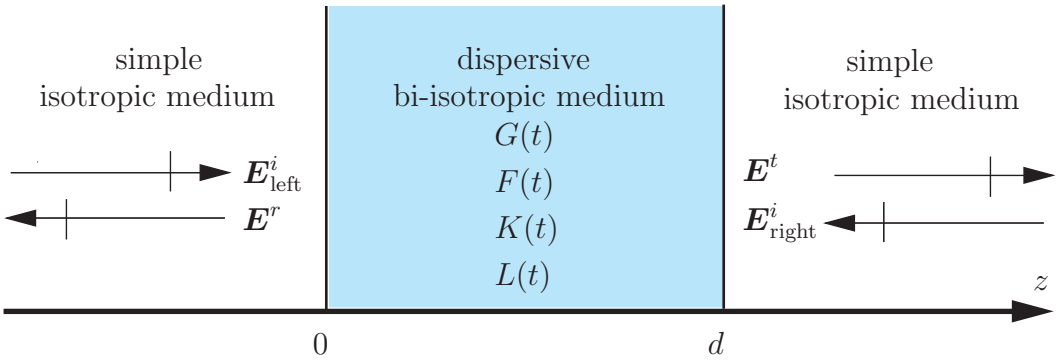

Figure 1: The infinite bi-isotropic scatterer. The up-going and down-going incident electric fields, $\boldsymbol{E}^i_{\rm left}(t-z/c)$ and $\boldsymbol{E}^i_{\rm right}(t+(z-d)/c)$, respectively, and the up-going and down-going scattered electric fields, $\boldsymbol{E}^t(t-z/c)$ and $\boldsymbol{E}^r(t+(z-d)/c)$, respectively, are indicated. In Sections 2–3, the down-going incident field is zero.

A general, up-going TEM wave is incident upon a homogeneous, temporally dispersive, bi-isotropic slab, $0<z<d$, for which the constitutive relations (2.1) are valid. The scattering geometry is depicted in Figure 1. For simplicity, the medium is located to vacuum for which $c\eta\boldsymbol{D}(\boldsymbol{r},t)=\boldsymbol{E}(\boldsymbol{r},t)$ and $c\boldsymbol{B}(\boldsymbol{r},t)=\eta\boldsymbol{H}(\boldsymbol{r},t)$. This means that the slab is optically impedance-matched. An extension to various optical mismatch cases can be found in Appendix B.

The incident electric field at the front wall, $z=0$, at time t is denoted by $\boldsymbol{E}^i_{\rm left}(t)$. This field is expected to be continuously differentiable and initially quiescent: it vanishes for $t<0$. The slab is supposed to be initially quiescent as well: the electric and magnetic fields vanish inside the bi-isotropic medium for $t<0$.

The Maxwell equations, $\nabla\times\boldsymbol{E}(\boldsymbol{r},t)=-\partial_t\boldsymbol{B}(\boldsymbol{r},t)$ and $\nabla\times\boldsymbol{H}(\boldsymbol{r},t)=\partial_t\boldsymbol{D}(\boldsymbol{r},t)$, support TEM-waves:

$$\boldsymbol{E}(\boldsymbol{r},t)=\boldsymbol{e}_xE_x(z,t)+\boldsymbol{e}_yE_y(z,t)\equiv\begin{pmatrix}E_x(z,t) & E_y(z,t)\end{pmatrix}^t.$$

The smooth input guarantees that there exists a unique TEM solution of Maxwell's equations in the space of continuous functions [17]. The solution is given explicitly below.

The reflected electric field at the front wall, $z=0$, at time t is denoted by $\boldsymbol{E}^r(t)$ and the transmitted electric field at the rear wall, $z=d$, at time t is $\boldsymbol{E}^t(t)$. In the direct scattering problem, the four susceptibility kernels are known and the scattered fields, $\boldsymbol{E}^r(t)$ and $\boldsymbol{E}^t(t)$, sought. In the inverse scattering problem, the scattered fields are known and the susceptibility kernels sought. It is understood that all these functions are restricted to an arbitrary but fixed compact time-interval, $0\le t\le T$. The space of continuous functions restricted to $0\le t\le T$ topologized by the maximum norm is denoted by $C[0,T]$.

2.2 The scattering relation

The solution of the propagation problem can be found in Ref. 16. In this reference, the slab is subjected to excitation from both sides. Double-sided excitation is superfluous in the inverse scattering problem for the bi-isotropic medium. Nevertheless, down-going waves are introduced in the present article. The reason for this is that these waves can be used theoretically to extend the obtained results to optically impedance-mismatched slabs, see Appendix B. The down-going incident electric field at the rear wall, $z = d$, at time t is denoted by $\boldsymbol{E}^i_{\text{right}}(t)$, see Figure 1. This field is assumed to be initially quiescent and continuously differentiable also.

To avoid cumbersome notation, the general time-dependence is (often) suppressed. The notation $\delta_a * E = E(t-a)$ for time-shift is used as well. Keeping this in mind, the scattering relation can be written in the form

$$\begin{pmatrix} \boldsymbol{E}^t \\ \boldsymbol{E}^r \end{pmatrix} = \begin{pmatrix} \mathcal{T}\delta_{\frac{d}{c}}* & \mathcal{R}^t \\ \mathcal{R} & \mathcal{T}^t\delta_{\frac{d}{c}}* \end{pmatrix} \begin{pmatrix} \boldsymbol{E}^i_{\text{left}} \\ \boldsymbol{E}^i_{\text{right}} \end{pmatrix}, \tag{2.2}$$

where the scattering operators $\mathcal{R}$, $\mathcal{R}^t$, $\mathcal{T}$, and $\mathcal{T}^t$ are matrix-valued temporal integral operators of type 2×2, and the superscript (t) refers to matrix transpose. These operators are independent of the excitation at the boundaries and depend on the susceptibility kernels of the medium only. The reflection and transmission operators can be written as

$$\mathcal{R} = \mathbf{R}*, \qquad \mathcal{T} = \mathbf{Q}(\mathbf{I} + \mathbf{T}*),$$

where the matrix-valued reflection and transmission kernels, $\mathbf{R}(t)$ and $\mathbf{T}(t)$, vanish for $t < 0$. In subsection 2.5, it is shown that these kernels are continuously differentiable except possibly at $t = 0$ and $t = d/c$. In component form,

$$\mathbf{R}(t) = \mathbf{I}R_{\text{co}}(t) + \mathbf{J}R_{\text{cross}}(t), \qquad \mathbf{T}(t) = \mathbf{I}T_{\text{co}}(t) + \mathbf{J}T_{\text{cross}}(t), \tag{2.3}$$

where

$$\mathbf{I} = \begin{pmatrix} 1 & 0 \\ 0 & 1 \end{pmatrix} \quad \text{and} \quad \mathbf{J} = \begin{pmatrix} 0 & -1 \\ 1 & 0 \end{pmatrix}.$$

The wave-front propagator of the slab is

$$\mathbf{Q} = \exp\left(-\frac{1}{c}\int_0^d \big(\mathbf{I}G(+0) + \mathbf{J}K(+0)\big)dz\right) = e^a(\mathbf{I}\cos\phi + \mathbf{J}\sin\phi),$$

where $a = -G(+0)d/c$ and $\phi = -K(+0)d/c$.

More exhaustively, the scattering operators in equation (2.2) can be written as

$$\begin{cases} \mathcal{R} = \mathcal{R}^\infty - \mathcal{M}\big(\mathcal{I} - \mathcal{R}^\infty(\mathcal{R}^\infty)^t\big)\mathcal{R}^\infty\delta_{2\frac{d}{c}} * \mathcal{P}\mathcal{P}^t, \\ \mathcal{T} = \mathcal{M}(\mathcal{I} - \mathcal{R}^\infty(\mathcal{R}^\infty)^t)\mathcal{P}, \end{cases} \tag{2.4}$$

where the matrix-valued temporal integral operators $\mathcal{R}^\infty$, $\mathcal{M}$, and $\mathcal{P}$ are linear combinations of the matrices $\mathbf{I}$ and $\mathbf{J}$. $\mathcal{I}$ is the 2×2 identity operator. The operator

identity (2.4) is the appropriate starting point for the direct as well as the inverse scattering problem. The integral operator

$$\mathcal{R}^\infty = \mathbf{R}^\infty *$$

is the reflection operator for the corresponding semi-infinite bi-isotropic medium, $0 < z < \infty$. The corresponding integral kernel,

$$\mathbf{R}^\infty(t) = \mathbf{I}R^\infty_{\rm co}(t) + \mathbf{J}R^\infty_{\rm cross}(t),$$

vanishes for $t < 0$. The operator $\mathcal{P}$ is the wave propagator for the bi-isotropic slab associated with up-going waves. This operator can be written in the form

$$\mathcal{P} = \mathbf{Q}(\mathbf{I} + \mathbf{P}*),$$

where the propagator kernel,

$$\mathbf{P}(t) = \mathbf{I}P_{\rm co}(t) + \mathbf{J}P_{\rm cross}(t),$$

vanishes for $t < 0$. Finally, the operator

$$\mathcal{M} = \big(\mathcal{I} - \delta_{2\frac{d}{c}} * \mathcal{R}^\infty(\mathcal{R}^\infty)^t\mathcal{P}\mathcal{P}^t\big)^{-1}$$

represents multiple propagation through the medium and multiple reflection at the boundaries of the medium. Notice that $\mathcal{M}$ is proportional to $\mathcal{I}$.

By the inverse $(1+f*)^{-1}$ of the convolution operator $1+f*$ is meant the integral operator $1 + f_{\rm res}*$, where $f_{\rm res}(t)$ is the resolvent kernel of the continuous kernel $f(t)$:

$$f(t) + f_{\rm res}(t) + (f * f_{\rm res})(t) = 0. \tag{2.5}$$

It is well-known that the resolvent equation (2.5) has a unique solution $f_{\rm res}(t)$ in $C[0,T]$. Furthermore, the resolvent kernel, $f_{\rm res}(t)$, depends continuously on data, $f(t)$, in the maximum norm. The series representation

$$f_{\rm res} = \sum_{n=1}^{\infty}(-1)^n(f*)^{n-1}f$$

can be employed to prove this fact, see Theorem A.1. The series expansion shows that $f_{\rm res}(t)$ is continuously differentiable if $f(t)$ is continuously differentiable. The resolvent equation is an example of a linear Volterra integral equation of the second kind. These equations are stable numerically.

In subsections 2.3–2.4, it is shown that the single-interface reflection kernel, $\mathbf{R}^\infty(t)$, is continuously differentiable except possibly at $t = 0$ and that the propagator kernel, $\mathbf{P}(t)$, is continuous except possibly at $t = 0$. Accordingly, the kernel of the operator $\mathcal{I} - \delta_{2\frac{d}{c}} * \mathcal{R}^\infty(\mathcal{R}^\infty)^t\mathcal{P}\mathcal{P}^t$ is continuous implying that $\mathcal{M}$ is well defined.

2.3 The refractive kernel and the single-interface reflection kernel

In terms of the susceptibility kernels, the reflection kernel for the semi-infinite medium, $\mathbf{R}^\infty(t)$, is

$$\mathbf{R}^\infty = -\left(\mathbf{I} + \frac{\mathbf{N}+\mathbf{G}}{2}*\right)^{-1}\frac{\mathbf{F}+\mathbf{L}}{2} = -\left(1 + \frac{N+G}{2}*\right)^{-1}\frac{\mathbf{F}+\mathbf{L}}{2}, \tag{2.6}$$

where the refractive kernel, $\mathbf{N}(t) = \mathbf{I}N(t)$, satisfies the non-linear integral Volterra equation of the second kind

$$2\mathbf{N} + \mathbf{N}*\mathbf{N} = 2\mathbf{G} + \mathbf{G}*\mathbf{G} - \mathbf{F}*\mathbf{F} + \mathbf{L}*\mathbf{L}, \tag{2.7}$$

and where $\mathbf{G}(t) = \mathbf{I}G(t)$, $\mathbf{K}(t) = \mathbf{J}K(t)$, $\mathbf{F}(t) = \mathbf{I}F(t)$, and $\mathbf{L}(t) = \mathbf{J}L(t)$. The components of the reflection kernel, $R^\infty_{\text{co}}(t)$ and $R^\infty_{\text{cross}}(t)$, satisfy the linear Volterra integral equations of the second kind

$$\begin{aligned} &2R^\infty_{\text{co}}(t) + (N * R^\infty_{\text{co}})(t) + (G * R^\infty_{\text{co}})(t) = F(t),\\ &2R^\infty_{\text{cross}}(t) + (N * R^\infty_{\text{cross}})(t) + (G * R^\infty_{\text{co}})(t) = L(t). \end{aligned} \tag{2.8}$$

The integral equation (2.7) has a unique solution in $C[0,T]$ and this solution depends continuously on susceptibility data, see Appendix A. Accordingly, $R^\infty_{\text{co}}(t)$ and $R^\infty_{\text{cross}}(t)$ are uniquely determined in $C[0,T]$ and depend continuously on susceptibility data. $N(t)$, $R^\infty_{\text{co}}(t)$, and $R^\infty_{\text{cross}}(t)$ vanish for $t<0$ and the series expansions show that these kernels are continuously differentiable in $[0,T]$ as well.

2.4 The wave propagator

The wave propagator, $\mathcal{P}$, can be written in the form

$$\mathcal{P} = \exp\left(\int_0^d \mathcal{G}\,dz\right) = \exp\left(\mathcal{G}d\right) = \mathbf{Q}(\mathbf{I} + \mathbf{P}*),$$

where the the temporal integral operator

$$\mathcal{G} = -\frac{1}{c}\frac{d}{dt}\big(\mathbf{N}+\mathbf{K}\big)* = -\frac{1}{c}\big(\mathbf{N}(+0)+\mathbf{K}(+0)\big) - \frac{1}{c}\big(\mathbf{N}'+\mathbf{K}'\big)*$$

is the generator of the wave propagator and $\mathbf{N}'(t)$ and $\mathbf{K}'(t)$ denote the classical time-derivatives of $\mathbf{N}(t)$ and $\mathbf{K}(t)$. Since numerical differentiation is ill-posed, the direct scattering problem is ill-posed. The wave propagator can be factored as

$$\mathcal{P} = \mathcal{P}_N\mathcal{P}_{\mathbf{K}}; \qquad \mathcal{P}_N = \exp\left(-\frac{d}{c}\partial_t N*\right), \quad \mathcal{P}_{\mathbf{K}} = \exp\left(-\frac{d}{c}\partial_t \mathbf{K}*\right),$$

where the exponentials are to be interpreted in terms of their power series, e.g.,

$$\exp\big(-\frac{d}{c}N'*\big) = 1 + \left(\sum_{n=1}^{\infty}\frac{1}{n!}\big(-\frac{d}{c}N'*\big)^{n-1}\big(-\frac{d}{c}N'\big)\right)* \tag{2.9}$$

Furthermore,

$$\exp\big(-\frac{d}{c}\mathbf{K}'*\big)=\mathbf{I}\cos\big(-\frac{d}{c}K'*\big)+\mathbf{J}\sin\big(-\frac{d}{c}K'*\big),$$

where the trigonometrical functions are

$$\cos\big(-\frac{d}{c}K'*\big)=1+\left(\sum_{n=1}^{\infty}\frac{(-1)^n}{(2n)!}\big(-\frac{d}{c}K'*\big)^{2n-1}\big(-\frac{d}{c}K'\big)\right)* \tag{2.10}$$

and

$$\sin\big(-\frac{d}{c}K'*\big)=\left(\sum_{n=0}^{\infty}\frac{(-1)^n}{(2n+1)!}\big(-\frac{d}{c}K'*\big)^{2n}\big(-\frac{d}{c}K'\big)\right)* \tag{2.11}$$

The kernels of the convolution operators (2.9)–(2.11) are series of continuous functions. According to Theorem A.1, these series converge uniformly in each compact time-interval, $0\le t\le T$. The limit functions are continuous and depend continuously on the functions $N'(t)$ and $K'(t)$. Consequently, the components of the propagator kernel, $P_{\rm co}(t)$ and $P_{\rm cross}(t)$, are uniquely determined in $C[0,T]$ and continuously dependent on data. By truncating the series, approximations to the propagator kernel can be obtained. $P_{\rm co}(t)$ and $P_{\rm cross}(t)$ vanish for $t<0$.

2.5 Direct scattering problem

The direct scattering problem can be summarized as follows: Starting with a set of continuously differentiable susceptibility kernels, $G(t)$, $K(t)$, $F(t)$, $L(t)$, $0\le t\le T$, the continuously differentiable refraction kernel, $N(t)$, $0\le t\le T$, is obtained by solving a non-linear Volterra integral equation of the second kind. $N(t)$ has a finite jump-discontinuity at $t=0$ if $G(t)$ is discontinuous at $t=0$. The continuously differentiable components of the reflection kernel for the semi-infinite medium, $R^{\infty}_{\rm co}(t)$, $R^{\infty}_{\rm cross}(t)$, $0\le t\le T$, can now be obtained by solving two linear Volterra integral equations of the second kind. $R^{\infty}_{\rm co}(t)$ has a finite jump-discontinuity at $t=0$ if $F(t)$ is discontinuous at $t=0$. Similarly, $R^{\infty}_{\rm cross}(t)$ is discontinuous at $t=0$ if $L(t)$ has a finite jump-discontinuity at $t=0$. In the next step, $N(t)$ and $K(t)$ are differentiated in classical sense. This is the only ill-posed step in the direct scattering problem. The components of the propagator kernel, $P_{\rm co}(t)$, $P_{\rm cross}(t)$, $0\le t\le T$, can then be obtained by equating series of temporal convolutions in terms of the continuous functions $N'(t)$ and $K'(t)$. $P_{\rm co}(t)$ and $P_{\rm cross}(t)$ are continuous except possibly at $t=0$, where they have finite jump-discontinuities if $N'(t)$ or $K'(t)$ have finite jump-discontinuities at $t=0$.

The reflection kernels, $R_{\rm co}(t)$, $R_{\rm cross}(t)$, $0\le t\le T$, and the transmission kernels, $T_{\rm co}(t)$ and $T_{\rm cross}(t)$, $0\le t\le T$, are computed roundtrip by roundtrip from equation (2.4). This equation can be written in the form

$$\begin{aligned}\mathcal{R}&=\mathcal{R}^{\infty}-\delta_{2\frac{d}{c}}*\mathcal{R}^{\infty}\big(\mathcal{I}-\mathcal{R}(\mathcal{R}^{\infty})^t\big)\mathcal{P}\mathcal{P}^t,\\ \mathcal{T}&=\big(\mathcal{I}-\mathcal{R}^{\infty}(\mathcal{R}^{\infty})^t\big)\mathcal{P}+\delta_{2\frac{d}{c}}*\mathcal{R}^{\infty}(\mathcal{R}^{\infty})^t\mathcal{P}\mathcal{P}^t\mathcal{T},\end{aligned} \tag{2.12}$$

where the first equation expresses $\mathcal{R}$ in $\mathcal{R}^\infty$ and $\mathcal{P}$ and the second gives $\mathcal{T}$ in terms of $\mathcal{R}^\infty$ and $\mathcal{P}$. The first roundtrip is the time-interval $0 < t < 2d/c$, the second $2d/c < t < 4d/c$, and so on. Obviously, $R_{\text{co}}(t)$ and $R_{\text{cross}}(t)$ are continuously differentiable except possibly at $t = 0$ and $t = 2d/c$, where they even may be discontinuous. $T_{\text{co}}(t)$ and $T_{\text{cross}}(t)$ are continuously differentiable except possibly at $t = 0$ and $t = 2d/c$. However, the transmission kernels are always continuous at $t = 2d/c$ (since the kernel of $\mathcal{R}^\infty(\mathcal{R}^\infty)^t$ is continuous). The reflection and transmission kernels are zero for $t < 0$. Finally, the reflected and transmitted fields are obtained by convolution of the scattering kernels and the incident electric field according to the scattering relation (2.2).

2.6 Preparations for the inverse scattering problem

Equation (2.4) is now examined further. First of all, since $\mathcal{R}^\infty(\mathcal{R}^\infty)^t$ is proportional to $\mathcal{I}$, the operators $\mathcal{R}(\mathcal{R}^\infty)^t$ and $\mathcal{P}^{-1}\mathcal{T}$ are proportional to $\mathcal{I}$. Secondly, by eliminating the multi-reflection operator, $\mathcal{M}$, the equation can be rewritten as

$$\begin{aligned} \mathcal{R} &= \mathcal{R}^\infty - \delta_{2\frac{d}{c}} * \mathcal{R}^\infty \mathcal{T} \mathcal{P}^t, \\ \mathcal{T} &= \big(\mathcal{I} - \mathcal{R}(\mathcal{R}^\infty)^t\big)\mathcal{P}. \end{aligned} \tag{2.13}$$

Actually, this system of equations appears in the process of deriving the scattering relation (2.2)–(2.4) above, see Ref. 16. Further manipulation leads to

$$\begin{aligned} (\mathcal{R}^\infty - \mathcal{R})(\mathcal{I} - \mathcal{R}^t\mathcal{R}^\infty) &= \delta_{2\frac{d}{c}} * \mathcal{R}^\infty \mathcal{T} \mathcal{T}^t, \\ \mathcal{T} &= (\mathcal{I} - \mathcal{R}\mathcal{R}^t)\mathcal{P} + \delta_{2\frac{d}{c}} * \mathcal{P}\mathcal{T}^t(\mathcal{T} - \mathcal{P}). \end{aligned} \tag{2.14}$$

These equations are appropriate for the inverse scattering problem. The first equation (2.14) expresses $\mathcal{R}^\infty$ in scattering data, $\mathcal{R}$ and $\mathcal{T}$. The second equation (2.14) gives $\mathcal{P}$ in terms of scattering data.

3 The inverse scattering problem

In this section, the theory of the inverse scattering problem is presented. All time-dependent functions are thought of as restrictions to the compact interval $0 \le t \le T$, where the upper limit T is arbitrary but fixed.

3.1 Problem formulation

In the inverse scattering problem, the properties of the medium are quantitatively unknown. In the process of recovering the four susceptibility kernels of the medium, the reflection and transmission kernels at normal incidence, (2.3), constitute data. The thickness of the slab d and the initial values $N(+0) = G(+0)$ and $K(+0)$ are assumed to be known *a priori*. These quantities determine the attenuation exponent, $a = -N(+0)d/c$, and the angle of rotation, $\phi = -K(+0)d/c$, which in

turn determine the wave-front propagator, **Q**. Physically, the most probable values are $G(+0) = K(+0) = 0$, see Ref. 6.

The scattering kernels, (2.3), are required to be continuous except possibly at one roundtrip, $t = 2d/c$, where jump-discontinuities in reflection data may be present:

$$\begin{aligned} R_{\mathrm{co}}(2d/c+0) - R_{\mathrm{co}}(2d/c-0) &= -e^{2a}R_{\mathrm{co}}(+0), \\ R_{\mathrm{cross}}(2d/c+0) - R_{\mathrm{cross}}(2d/c-0) &= -e^{2a}R_{\mathrm{cross}}(+0). \end{aligned} \tag{3.1}$$

The aim is to reconstruct at least continuous susceptibility kernels can be generated.

In practise, data — also the function values $K(+0)$ and $G(+0)$ — are obtained by deconvolution of the scattered electric fields, $\boldsymbol{E}^r(t)$ and $\boldsymbol{E}^t(t)$, with respect to the incident electric field, $\boldsymbol{E}^i_{\mathrm{left}}(t)$, see equation (2.2). At this step, the condition (3.1) can be satisfied without major difficulty. Experience shows that by choosing sharp incident pulses, trivial deconvolution techniques can be employed [15]. It should be remarked that the angle of rotation, ϕ, cannot be determined uniquely. However, since the effects of chirality are believed to be small, it is reasonable to assume that $|\phi| < \pi/2$, which leads to a unique value of $K(+0)$.

It is well known that deconvolution is an ill-posed problem. The aim of the present analysis is to show that the deconvolution of the scattered electric fields is the only ill-posed step of the inverse problem. In other words, the inverse scattering problem based on generic data is well posed.

In the sense of Hadamard, the (generic) inverse scattering problem is well posed if the following criteria are fulfilled:
(1) There exists a set of susceptibility kernels $G(t)$, $K(t)$, $F(t)$, $L(t)$, $0 \le t \le T$ for each set of scattering kernels $R_{\mathrm{co}}(t)$, $R_{\mathrm{cross}}(t)$, $T_{\mathrm{co}}(t)$, $T_{\mathrm{cross}}(t)$, $0 \le t \le T$.
(2) The solution (the set of susceptibility kernels) is uniquely determined by data (the set of scattering kernels).
(3) The solution depends continuously on data.
It is understood that the function space of continuous functions furnished with the maximum norm has been chosen. Since the reflection kernel is discontinuous at one roundtrip $2d/c$, this statement is ambiguous if the time-interval is longer that one roundtrip, that is, if $T > 2d/c$. This problem can be solved by splitting the interval in two disjoint intervals, $0 \le t \le 2d/c$ and $2d/c \le t \le T$, and treat the problems restricted to these intervals separately, beginning with the first. In the sequel, this division is always understood.

Below, the inverse scattering problem for the bi-isotropic slab is solved step by step using the concepts introduced in previous sections. It is shown that the conditions (1)–(3) hold at each of these steps. It should be observed that each of the steps can be performed also in practise; therefore, the theory presented in this section constitutes a new inverse method of obtaining the susceptibility kernels of an isotropic or bi-isotropic medium from generic scattering data at normal incidence. Notice that the new method can be combined with the Green functions method for the non-reflective (non-coupling) medium [9, 15].

3.2 Solution of the inverse problem

First of all, introduce a scalar transmission operator $\mathcal{T}_s$ by $\mathcal{T}_s\mathcal{I} := \mathcal{P}_{\mathbf{K}}^{-1}\mathcal{T}$. The definition is equivalent to the system of operator equations

$$\begin{aligned}\mathcal{T}_s &= e^a(1+T_{\mathrm{co}}*)\cos\left(-\frac{d}{c}K'*\right) + e^a T_{\mathrm{cross}} * \sin\left(-\frac{d}{c}K'*\right),\\ 0 &= e^a(1+T_{\mathrm{co}}*)\sin\left(-\frac{d}{c}K'*\right) - e^a T_{\mathrm{cross}} * \cos\left(-\frac{d}{c}K'*\right),\end{aligned} \tag{3.2}$$

where the second identity is used to determine the time-derivative of the chirality kernel. In Appendix A, it is proven that $K'(t)$ is uniquely determined by the transmission kernels in the space of continuous functions furnished with the maximum norm. Moreover, it is shown that it depends continuously on these functions. Thus, the reconstruction of the continuous kernel $K'(t)$ is well posed. Explicitly, the solution is

$$-\frac{d}{c}K'* = \arctan\left(T_{\mathrm{quotient}}*\right), \tag{3.3}$$

where the kernel $T_{\mathrm{quotient}} = (1+T_{\mathrm{co}}*)^{-1}T_{\mathrm{cross}}$ is continuous and continuously dependent on transmission data and the right-hand side is interpreted as a convolution operator with the continuous kernel

$$\sum_{n=0}^{\infty}\frac{(-1)^n}{2n+1}(T_{\mathrm{quotient}}*)^{2n}T_{\mathrm{quotient}}.$$

The differentiable chirality kernel is readily obtained by integration of $K'(t)$. Since the integration constant is uniquely determined by the *a priori* knowledge of $K(+0)$, the reconstruction of $K(t)$ is well posed.

The integral kernel $T_s(t)$ of the operator $\mathcal{T}_s = e^a(1+T_s*)$ can now be obtained by definition (3.2). According to Theorem A.1, the operators $\cos\left(-\frac{d}{c}K'*\right)$ and $\sin\left(-\frac{d}{c}K'*\right)$ have continuous kernels, which depend continuously on $K'(t)$. Therefore, $T_s(t)$ becomes continuous and continuously dependent on transmission data. In other words, the construction of the kernel $T_s(t)$ is well posed. $T_s(t)$ can be obtained by solving the non-linear Volterra integral equation of the second kind

$$2T_s(t) + (T_s * T_s)(t) = 2T_{\mathrm{co}}(t) + (T_{\mathrm{co}} * T_{\mathrm{co}})(t) + (T_{\mathrm{cross}} * T_{\mathrm{cross}})(t), \tag{3.4}$$

which follows from the operator equality $\cos^2\left(-\frac{d}{c}K'*\right) + \sin^2\left(-\frac{d}{c}K'*\right) = 1$.

As a consequence of definition (3.2), the second integral equation (2.14) reduces to the scalar operator equation $\mathcal{T}_s = (1-\mathcal{R}_s^2)\mathcal{P}_N + \delta_{2\frac{d}{c}} * \mathcal{P}_N\mathcal{T}_s(\mathcal{T}_s - \mathcal{P}_N)$ or

$$\mathcal{P}_N = (1-\mathcal{R}_s^2)^{-1}\mathcal{T}_s - \delta_{2\frac{d}{c}} * (1-\mathcal{R}_s^2)^{-1}\mathcal{P}_N\mathcal{T}_s(\mathcal{T}_s - \mathcal{P}_N), \tag{3.5}$$

where the scalar reflection operator $\mathcal{R}_s^2$, defined by $\mathcal{R}_s^2\mathcal{I} := \mathcal{R}\mathcal{R}^t = \mathbf{I}R_s^2*$, has the continuous kernel

$$R_s^2(t) := (R_{\mathrm{co}} * R_{\mathrm{co}})(t) + (R_{\mathrm{cross}} * R_{\mathrm{cross}})(t), \tag{3.6}$$

Obviously, the scalar propagator kernel, $P_N(t)$, defined by $\mathcal{P}_N = e^a(1 + P_N*)$, can be obtained roundtrip by roundtrip by direct computation. Since the scalar transmission kernel $T_s(t)$ and the resolvent kernel of $R_s^2(t)$ are continuous and depend continuously on data, it follows that $P_N(t)$ has these properties. The continuity at $2d/c$ is implied by the fact that $P_N(+0) = T_s(+0)$.

Once the continuous kernel $P_N(t)$ has been obtained, the time-derivative of the refractive kernel, $N'(t)$, is recovered from the operator equation

$$\mathcal{P}_N = e^a \exp\big(-\frac{d}{c}N'*\big). \tag{3.7}$$

In Appendix A, it is shown that $N'(t)$ is uniquely determined by $P_N(t)$ in the space of continuous functions furnished with the maximum norm, and, in addition, that it depends continuously on $P_N(t)$ — that is, scattering data — in this norm. The solution of the operator equation reads

$$-\frac{d}{c}N'* = \ln(1 + P_N*), \tag{3.8}$$

where the right-hand side is interpreted as a convolution operator with the continuous kernel

$$-\sum_{n=1}^{\infty}\frac{(-1)^n}{n}(P_N*)^{n-1}P_N.$$

The refraction kernel, $N(t)$, is obtained from $N'(t)$ by integration. This step is well posed, since the constant of integration is uniquely determined by the *a priori* know-ledge of $N(+0) = G(+0)$. Consequently, the construction of the differentiable kernel $N(t)$ from scattering data is well posed.

Since $\mathcal{T}_s$ and $\mathcal{P}_N$ are known operators, the scalar components, $\mathcal{R}_{\rm co}^{\infty} = R_{\rm co}^{\infty}*$ and $\mathcal{R}_{\rm cross}^{\infty} = R_{\rm cross}^{\infty}*$, of the reflection operator for the corresponding semi-infinite medium, $\mathcal{R}^{\infty} = \mathbf{R}^{\infty}*$, can be obtained roundtrip by roundtrip by employing the first equation (2.13):

$$\begin{cases} \mathcal{R}_{\rm co}^{\infty} = \mathcal{R}_{\rm co} + \delta_{2\frac{d}{c}} * \mathcal{R}_{\rm co}^{\infty}\mathcal{T}_s\mathcal{P}_N, \\ \mathcal{R}_{\rm cross}^{\infty} = \mathcal{R}_{\rm cross} + \delta_{2\frac{d}{c}} * \mathcal{R}_{\rm cross}^{\infty}\mathcal{T}_s\mathcal{P}_N. \end{cases} \tag{3.9}$$

Due to these equations and the condition (3.1), the reflection kernels $R_{\rm co}^{\infty}(t)$ and $R_{\rm cross}^{\infty}(t)$ are uniquely determined continuous functions, which depend continuously on data. In other words, the reconstruction of these functions is a well posed problem.

The susceptibility kernel $G(t)$ is obtained next. This is accomplished by substituting equation (2.6) into equation (2.7), resulting in

$$\big(2 + (N+G)*\big)\Big(N - G - \big(2 + (N+G)*\big)\big(R_{\rm co}^{\infty} * R_{\rm co}^{\infty} + R_{\rm cross}^{\infty} * R_{\rm cross}^{\infty}\big)\Big) = 0,$$

and, consequently,

$$N - G - \big(2 + (N+G)*\big)\big(R_{\rm co}^{\infty} * R_{\rm co}^{\infty} + R_{\rm cross}^{\infty} * R_{\rm cross}^{\infty}\big) = 0. \tag{3.10}$$

This identity is a linear Volterra equation of the second kind in $G(t)$. Since $N(t)$ and $(R^{\infty}_{\rm co} * R^{\infty}_{\rm co} + R^{\infty}_{\rm cross} * R^{\infty}_{\rm cross})(t)$ are continuous and depend continuously on data, $G(t)$ inherit these properties. Hence, the reconstruction of the susceptibility kernel $G(t)$ is well posed. Finally, the kernels $F(t)$ and $L(t)$ are obtained from the equations (2.6) by direct computation. Clearly, the reconstruction of these kernels is well posed.

3.3 An alternative numerical procedure

Natural optically active media have resonance frequencies in the optical regime. For these materials, the infinite series approach developed in previous sections may not effective enough numerically. In this subsection, an alternative technique is presented. In particular, this method is advantageous in the inverse scattering problem when the refractive kernel is to be obtained from the propagator kernel. However, the technique works in the direct scattering problem as well.

Knowing the propagator kernel, $\mathbf{P}(t)$, a linear Volterra integral equation of the second kind can then be solved for the kernel $t(\mathbf{N}'(t) + \mathbf{K}'(t))$:

$$t\mathbf{P} = -dc^{-1}t(\mathbf{N}' + \mathbf{K}') - dc^{-1}\left(t(\mathbf{N}' + \mathbf{K}')\right) * \mathbf{P}. \tag{3.11}$$

This equation can be obtained by multiplying the series expansion of $\mathbf{P}(t)$ by t and using the general identity for causal convolutions

$$t\,\frac{\overbrace{(f * \ldots * f)}^{k \text{ functions}}}{k!} = (tf) * \frac{\overbrace{(f * \ldots * f)}^{k-1 \text{ functions}}}{(k-1)!}, \qquad k > 1. \tag{3.12}$$

This latter equality is easily proved by mathematical induction. Observe that equation (3.11) is a linear Volterra integral equation of the second kind in the propagator kernel as well. Knowing $\mathbf{N}'(t)$ and $\mathbf{K}'(t)$, $\mathbf{P}(t)$ can be determined.

Practically, the inverse scattering problem can be solved in the following way. The product $tK'(t)$ can be obtained directly from transmission data by solving the linear Volterra integral equation of the second kind

$$tT_{\rm quotient} = -dc^{-1}\{tK' + (tK') * T_{\rm quotient} * T_{\rm quotient}\}. \tag{3.13}$$

The kernel $T_{\rm quotient}(t)$ satisfies another linear Volterra integral equation of the second kind:

$$T_{\rm quotient}(t) + (T_{\rm co} * T_{\rm quotient})(t) = T_{\rm cross}(t)$$

Equation (3.13) is obtained by applying the rule (3.12) to the expansion (3.3). The scalar transmission kernel, $T_s(t)$, is obtained from transmission data by solving the non-linear Volterra integral equation of the second kind (3.4). The scalar reflection kernel, $R^2_s(t)$, is obtained from equation (3.6) by straightforward convolution of reflection data. Equation (3.5) can be written in the form

$$\begin{aligned} P_N(t) + (R^2_s * P_N)(t) &= T_s(t) - R^2_s(t) + e^{2a}\left\{P^2_N(t - 2d/c) - T^2_s(t - 2d/c)\right\} + \\ &+ e^{2a}\left\{(T_s * P^2_N)(t - 2d/c) - (T^2_s * P_N)(t - 2d/c)\right\}, \end{aligned}$$

where $T_s^2(t) = (T_s * T_s)(t)$ and $P_N^2(t) = (P_N * P_N)(t)$. This delayed Volterra equation of the second kind is solved for the propagator kernel $P_N(t)$. Using the expansion (3.8) and the rule (3.12), it can be shown that the product $tN'(t)$ satisfies the linear Volterra integral equation of the second kind

$$tP_N = -dc^{-1}\{tN' + (tN') * P_N\}. \tag{3.14}$$

Knowing the products $tN'(t)$ and $tK'(t)$, the kernels $N(t)$ and $K(t)$ are obtained by straightforward integration. The delayed equations (3.9) are solved for the reflection kernels for the half-space, $R_{\rm co}^{\infty}(t)$ and $R_{\rm cross}^{\infty}(t)$:

$$\begin{aligned} R_{\rm co}^{\infty}(t) &= R_{\rm co}(t) + e^{2a}\left\{(S * R_{\rm co}^{\infty})(t-2d/c) + R_{\rm co}^{\infty}(t-2d/c)\right\}, \\ R_{\rm cross}^{\infty}(t) &= R_{\rm cross}(t) + e^{2a}\left\{(S * R_{\rm co}^{\infty})(t-2d/c) + R_{\rm cross}^{\infty}(t-2d/c)\right\}, \end{aligned}$$

where $S(t) = P_N(t) + (T_s * P_N)(t) + T_s(t)$. Finally, $G(t)$ is determined by solving the linear Volterra integral equation of the second kind (3.10), whereas $F(t)$ and $L(t)$ are obtained from equations (2.6) by convolution. Naturally, several of these steps can be modified and carried out in another order.

As an example, consider the multi-resonance medium discussed in Ref. 9:

$$\begin{aligned} G(t) &= 0.5e^{-0.2t}\sin 5t + 0.25e^{-0.5t}\sin 10t, & K(t) &= 0.01e^{-0.5t}\cos 10t, \\ F(t) &= 0.5e^{-0.2t}\sin 5t + 0.2e^{-0.5t}\sin 10t, & L(t) &= 0. \end{aligned}$$

In this case, $R_{\rm cross}(t) = 0$ and $R(t) := R_{\rm co}(t)$. The susceptibility kernels, $G(t)$, $K(t)$, and $F(t)$, and their reconstructions are shown in Figure 2. Scattering data, $R(t)$, $T_{\rm co}(t)$, and $T_{\rm cross}(t)$, has been generated using series expansions and is displayed in Figure 3. The reconstructions have been obtained by solving a number of Volterra integral equations of the second kind, see the previous paragraph. 128 points per roundtrip is used in this example.

4 Conclusion

It has been shown, that the inverse scattering problem of recovering the four differentiable susceptibility kernels of the bi-isotropic slab $G(t)$, $K(t)$, $F(t)$, $L(t)$, $0 \le t \le T$ from generic scattering data at normal incidence $R_{\rm co}(t)$, $R_{\rm cross}(t)$, $T_{\rm co}(t)$, $T_{\rm cross}(t)$, $0 \le t \le T$ is well posed in the sense of Hadamard, using the space of continuous functions subject to the maximum norm. In the process of reconstruction, the initial values $G(+0)$ and $K(+0)$ are assumed to be known. Examples of fine reconstructions have been published before [15], and an alternative, more efficient, numerical method is accounted for in the present article. The theoretical results in this article support these inverse algorithms: the deconvolution of the scattered fields is the only ill-posed step in the time-domain inverse algorithm.

Appendix A Proofs of well-posedness

This appendix contains several proofs. First a general theorem applicable to both the direct and inverse scattering problems is presented and proved. The second

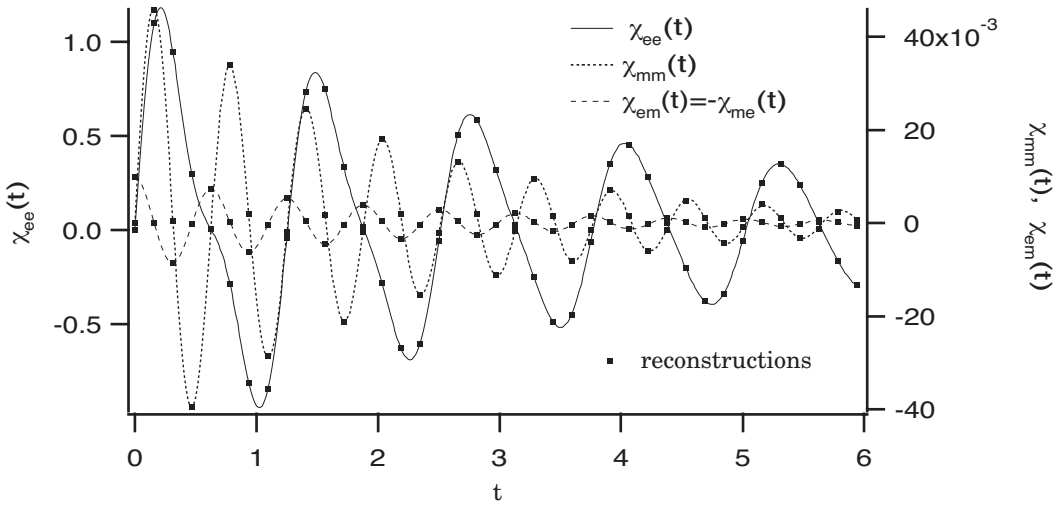

Figure 2: The electric susceptibility kernel, $\chi_{ee}(t)$, the magnetic susceptibility kernel, $\chi_{mm}(t)$, and the chirality kernel, $\chi_{em}(t) = -\chi_{me}(t)$, for a reciprocal multi-resonance medium in units of c/d. Time t is measured in units of d/c.

proof of this section is relevant for the direct problem, whereas the remaining ones concern the inverse scattering problem.

The theorem reads:

Theorem A.1. *Let $(a_n)_{n=1}^{\infty}$ be an arbitrary but fixed sequence of bounded real numbers. If f is a real continuous function defined in the real compact interval $[0,T]$, then the function series of causal convolutions*

$$[0,T] \ni t \to \sum_{k=1}^{\infty} a_k \big((f*)^{k-1} f\big)(t) \tag{A.1}$$

converges uniformly in $[0,T]$ to a continuous function. The limit function F depends continuously on f in maximum norm $\|f\|_\infty = \max_{0\le t\le T} |f(t)|$.

The causal convolution of the functions $[0,T] \ni t \to f(t)$ and $[0,T] \ni t \to g(t)$ is defined by the function

$$[0,T] \ni t \to (f*g)(t) := \int_0^t f(t-t')g(t')\,dt'.$$

Moreover, $(f*)^0 := 1$, $(f*)^1 := f*$, $(f*)^2 := (f*f)*$, and so on. The proof of the theorem is elementary:

Proof. Let the sequence a_n be bounded by C. By induction one shows that the functions $(f*)^{k-1}f$, $k = 1, 2, 3, \ldots$ are continuous and that

$$|\big((f*)^{k-1}f\big)(t)| \le \frac{t^{k-1}}{(k-1)!}(\|f\|_\infty)^k, \qquad 0 \le t \le T, \qquad k = 1, 2, 3, \ldots.$$

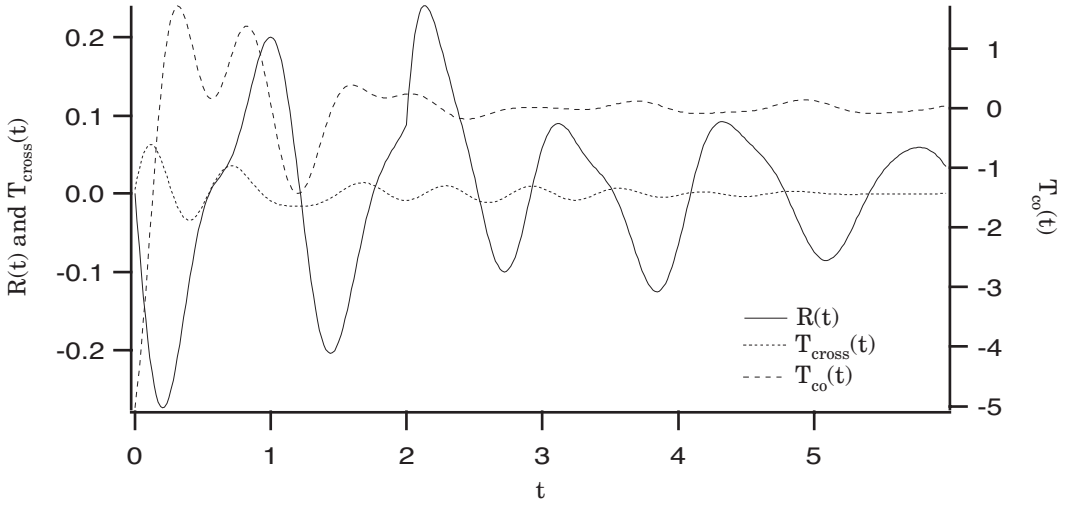

Figure 3: The scattering kernels $R(t)$, $T_{\rm co}(t)$, and $T_{\rm cross}(t)$ in units of c/d. Time t is measured in units of d/c.

Since the numerical series

$$C\sum_{k=1}^{\infty}\frac{T^{k-1}}{(k-1)!}(\|f\|_\infty)^k$$

converges, the first part of the theorem is a direct consequence of the Weierstrass test.

In order to prove the continuous dependence, let f be fixed and $\epsilon>0$ arbitrary. Furthermore, let g be any continuous function in $[0,T]$ such that $\|f-g\|_\infty<\epsilon$, and denote by G the limit function associated with the sequence $(a_n)_{n=1}^\infty$ and the function g. Straightforward calculations show that

$$F-G=(a_1+h*)(f-g),$$

where the function h is

$$h=\sum_{n=2}^{\infty}a_n\big((f*)^{n-2}f+(f*)^{n-2}g+\ldots+(g*)^{n-2}f+(g*)^{n-2}g\big).$$

Since the terms of this series can be estimated by

$$C\frac{nt^{n-2}}{(n-2)!}(\|f\|_\infty+\epsilon)^{n-1},\qquad 0\le t\le T,$$

the function h is continuous by the Weierstrass test. Consequently, for fixed f and arbitrary $\epsilon>0$,

$$\begin{aligned}\|F-G\|_\infty &\le C\left(1+\sum_{n=0}^{\infty}\frac{(n+2)T^{n+1}}{(n+1)!}(\|f\|_\infty+\epsilon)^{n+1}\right)\epsilon=\\ &=Ce^{T(\|f\|_\infty+\epsilon)}\big(1+T(\|f\|_\infty+\epsilon)\big)\epsilon\end{aligned}$$

if only $\|f-g\|_\infty<\epsilon$. This completes the proof.

A.1 Construction of the refractive kernel

Proposition. Given susceptibility data, equation (2.7) has a unique solution $N(t)$, $0 \le t \le T$ in the space of continuous functions furnished with the maximum norm. The solution depends continuously on data. Consequently, the construction of the refractive kernel from susceptibility data is well posed.

Proof. The solution is given explicitly by

$$N = \sum_{k=1}^{\infty} \binom{\frac{1}{2}}{k} (\chi *)^{k-1} \chi, \tag{A.2}$$

where the function

$$\chi = 2G + G * G - F * F - L * L$$

is continuous and continuously dependent on susceptibility data. By Theorem A.1, this solution is continuous.

The solution (A.2) is unique in the space of continuous functions furnished with the maximum norm. For if $N_1(t)$, $0 \le t \le T$ is another continuous solution, then

$$\left(1 + \frac{(N + N_1)}{2} *\right) \big(N - N_1\big) = 0, \qquad 0 \le t \le T.$$

This is a homogeneous linear Volterra integral equation of the second kind in the continuous function $N - N_1$ with continuous kernel $N + N_1$. Unique solubility of these equations yields that $N(t) = N_1(t)$ for $0 \le t \le T$.

According to Theorem A.1, the representation (A.2) establishes the continuous dependence on susceptibility data. This completes the proof.

A.2 Reconstruction of time derivative of the chirality kernel

Proposition. The second equation (3.2) has a unique solution $-d/cK'(t)$, $0 \le t \le T$ in the space of continuous functions furnished with the maximum norm, and this solution depends continuously on data $T_{\text{quotient}}(t)$, $0 \le t \le T$. In other words, the reconstruction of the time derivative of the chirality kernel from transmission data is well posed.

Proof. The solution is explicitly given by equation (3.3) and is continuous by Theorem A.1.

The solution is unique in the space of continuous functions furnished with the maximum norm. For if $-d/cK_1'(t)$, $0 \le t \le T$ is another continuous solution, then

$$\left(\cos\left(-\frac{d}{c}K' *\right)\right)^{-1} \sin\left(-\frac{d}{c}K' *\right) = T_{\text{quotient}} = \left(\cos\left(-\frac{d}{c}K_1' *\right)\right)^{-1} \sin\left(-\frac{d}{c}K_1' *\right),$$

which can be written in the form

$$\sin\left(\Delta *\right) = \sum_{k=0}^{\infty} \frac{(-1)^k}{(2k+1)!} (\Delta *)^{2k+1} = 0, \qquad \Delta(t) = -\frac{d}{c}\big(K'(t) - K_1'(t)\big),$$

or

$$\left(1+\sum_{k=1}^{\infty}\frac{(-1)^k}{(2k+1)!}(\Delta*)^{2k}\right)\Delta=0. \tag{A.3}$$

Since $\Delta(t)$ is continuous by definition, Theorem A.1 shows that equation (A.3) is a homogeneous, linear Volterra integral equation of the second kind in $\Delta(t)$ with continuous kernel. Consequently, $\Delta(t)=0$, $0\le t\le T$, that is, $K_1'(t)=K'(t)$, $0\le t\le T$.

According to Theorem A.1, the representation (3.3) establishes the continuous dependence on transmission data. This finishes the proof.

Alternatively, one can use that equation (3.13) is a linear Volterra integral equation of the second kind in the kernel $tK'(t)$.

A.3 Reconstruction of time derivative of the refractive kernel

Proposition. Equation (3.7) has a unique solution $-d/cN'(t)$, $0\le t\le T$ in the space of continuous functions furnished with the maximum norm, and this solution depends continuously on data $P_N(t)$, $0\le t\le T$. In other words, the reconstruction of $N'(t)$ from scattering data is well posed.

Proof. The solution is given explicitly by equation (3.8), and by Theorem A.1, it is continuous.

The solution is unique in the space of continuous functions furnished with the maximum norm. For if $-d/cN_1'(t)$, $0\le t\le T$ is another continuous solution, then

$$(1+h*)\Delta=0,\qquad \Delta(t)=-\frac{d}{c}\big(N'(t)-N_1'(t)\big). \tag{A.4}$$

where

$$h=\sum_{n=2}^{\infty}\frac{1}{n!}\big((f*)^{n-2}f+(f*)^{n-2}g+\ldots+(g*)^{n-2}f+(g*)^{n-2}g\big),$$

$f(t)=-\frac{d}{c}N'(t)$, and $g(t)=-\frac{d}{c}N_1'(t)$. Since the terms of the series expansion of the kernel $h(t)$ can be estimated by

$$\frac{t^{n-2}}{(n-1)!(n-2)!}(\|f\|_\infty+\|g\|_\infty)^{n-1},\qquad 0\le t\le T,$$

this function is continuous by the Weierstrass test. Consequently, equation (A.4) is a homogeneous, linear Volterra integral equation of the second kind in $\Delta(t)$ with continuous kernel $h(t)$. Hence, $\Delta(t)=0$, $0\le t\le T$, that is, $N_1'(t)=N'(t)$, $0\le t\le T$.

According to Theorem A.1, the representation (3.8) establishes the continuous dependence on scattering data, which finishes the proof.

Alternatively, one can use the series equation (3.14) to prove the theorem.

Appendix B Optical impedance mismatch

In this appendix, the general mismatch-problem for the dispersive bi-isotropic slab is discussed. The obtained results are useful in the inverse as well as in the direct scattering problem.

One way to cope with the complexity of the general mismatch-problem is to use the explicit scattering relation derived in Ref. 16. This approach is straightforward. Alternatively, the problem can be reduced to the one studied in previous sections. This indirect approach is discussed below.

The reduction is carried out in two steps, referring to the principle of superposition in both. Similar results have been obtained for the stratified, nonmagnetic isotropic slab by Kristensson and Krueger [8] using so called Redheffer star products [14].

B.1 Basic equations

Consider the dynamical equation of the dispersive bi-isotropic medium defined by the constitutive relations (2.1):

$$\begin{pmatrix}(c\partial_z+\partial_t)\boldsymbol{E}^+\\(c\partial_z-\partial_t)\boldsymbol{E}^-\end{pmatrix}=\partial_t\left\{\begin{pmatrix}-\mathbf{G}-\mathbf{K} & -\mathbf{F}+\mathbf{L}\\ \mathbf{F}+\mathbf{L} & \mathbf{G}-\mathbf{K}\end{pmatrix}*\begin{pmatrix}\boldsymbol{E}^-, & \boldsymbol{E}^+\\ & 0\le z\le d.\end{pmatrix}\right\}. \quad \text{(B.1)}$$

The split vector fields $\boldsymbol{E}^{\pm}(z,t)$ are the dependent variables of the wave-propagation problem. These are related to the electric and magnetic fields through an optical wave splitting, see Ref. 16. The boundary conditions at the front and the rear walls are

$$\begin{pmatrix}\boldsymbol{E}^i_{\text{left}}(t)\\ \boldsymbol{E}^r(t)\end{pmatrix}=\frac{1}{1+r_0}\begin{pmatrix}\mathbf{I} & r_0\mathbf{I}\\ r_0\mathbf{I} & \mathbf{I}\end{pmatrix}\begin{pmatrix}\boldsymbol{E}^+(+0,t)\\ \boldsymbol{E}^-(+0,t)\end{pmatrix} \quad \text{(B.2)}$$

and

$$\begin{pmatrix}\boldsymbol{E}^t(t)\\ \boldsymbol{E}^i_{\text{right}}(t)\end{pmatrix}=\frac{1}{1+r_1}\begin{pmatrix}\mathbf{I} & r_1\mathbf{I}\\ r_1\mathbf{I} & \mathbf{I}\end{pmatrix}\begin{pmatrix}\boldsymbol{E}^+(d-0,t)\\ \boldsymbol{E}^-(d-0,t)\end{pmatrix}, \quad \text{(B.3)}$$

respectively, where

$$r_0=\frac{\eta(+0)-\eta(-0)}{\eta(+0)+\eta(-0)} \quad \text{and} \quad r_1=\frac{\eta(d-0)-\eta(d+0)}{\eta(d-0)+\eta(d+0)}$$

are the optical reflection coefficients viewed from the surrounding non-dispersive isotropic media. $\boldsymbol{E}^i_{\text{left}}(t)$ and $\boldsymbol{E}^i_{\text{right}}(t)$ are the right-going and left-going incident electric fields measured at the walls, and the corresponding scattered electric fields are $\boldsymbol{E}^s_{\text{left}}(t)=\boldsymbol{E}^r(t)$ and $\boldsymbol{E}^s_{\text{right}}(t)=\boldsymbol{E}^t(t)$, respectively, see Figure 1. The intrinsic impedance of the medium to the left of the slab is denoted by $\eta(-0)$ and the corresponding property of the medium to the right is $\eta(d+0)$. Moreover,

$$\eta=\eta(+0)=\eta(d-0),$$

since the slab is homogeneous, see the constitutive relations (2.1). The optically impedance-matched slab is characterized by $r_0=r_1=0$.

Notice that equation (B.3) holds for a metal-backed (PEC-backed) slab as well. In this case, $r_1 = 1$ independent of optical intrinsic impedance η of the slab.

The investigation in Ref. 16 shows that the general scattering relation can be written in the operator form

$$\begin{pmatrix} \boldsymbol{E}^s_{\text{right}} \\ \boldsymbol{E}^s_{\text{left}} \end{pmatrix} = \begin{pmatrix} \mathcal{T}_{\text{left}}\delta_{\frac{d}{c}}* & \mathcal{R}_{\text{right}} \\ \mathcal{R}_{\text{left}} & \mathcal{T}_{\text{right}}\delta_{\frac{d}{c}}* \end{pmatrix} \begin{pmatrix} \boldsymbol{E}^i_{\text{left}} \\ \boldsymbol{E}^i_{\text{right}} \end{pmatrix}, \tag{B.4}$$

where the introduced reflection and transmission integral operators are

$$\begin{cases} \mathcal{T}_{\text{left}} = (1+r_0)(1-r_1)\mathbf{Q}^+\Big(\big(\mathbf{I} - r_0 r_1 \mathbf{Q}^+\mathbf{Q}^-\delta_{\frac{2d}{c}}*\big)^{-1} + \mathbf{T}_{\text{left}}*\Big) \\ \mathcal{R}_{\text{left}} = r_0\mathbf{I} - (1-r_0^2)r_1\mathbf{Q}^+\mathbf{Q}^-\big(\mathbf{I} - r_0 r_1 \mathbf{Q}^+\mathbf{Q}^-\delta_{\frac{2d}{c}}*\big)^{-1}\delta_{\frac{2d}{c}}* + (1-r_0^2)\mathbf{R}_{\text{left}}* \\ \mathcal{T}_{\text{right}} = (1-r_0)(1+r_1)\mathbf{Q}^-\Big(\big(\mathbf{I} - r_0 r_1 \mathbf{Q}^+\mathbf{Q}^-\delta_{\frac{2d}{c}}*\big)^{-1} + \mathbf{T}_{\text{right}}*\Big) \\ \mathcal{R}_{\text{right}} = r_1\mathbf{I} - (1-r_1^2)r_0\mathbf{Q}^+\mathbf{Q}^-\big(\mathbf{I} - r_0 r_1 \mathbf{Q}^+\mathbf{Q}^-\delta_{\frac{2d}{c}}*\big)^{-1}\delta_{\frac{2d}{c}}* + (1-r_1^2)\mathbf{R}_{\text{right}}* \end{cases}$$

where $\mathbf{Q}^+ = \mathbf{Q}$ and $\mathbf{Q}^- = \mathbf{Q}^t$ (matrix transpose).

B.2 Decomposition of the problem

The following wave-propagation problem is now discussed:

- **Problem.** Find the solution $\boldsymbol{E}^{\pm}(z,t)$ of the dynamical equation (B.1) subject to the boundary conditions

$$\begin{cases} \boldsymbol{E}^i(t) = \dfrac{1}{1+r_0}\big(\boldsymbol{E}^+(+0,t) + r_0\boldsymbol{E}^-(+0,t)\big), \\ \boldsymbol{E}^-(d-0,t) = -r_1\boldsymbol{E}^+(d-0,t). \end{cases}$$

  This is the full mismatch problem ($r_0 \neq 0$, $r_1 \neq 0$), but the excitation from the right is zero ($\boldsymbol{E}^i_{\text{right}}(t) = \mathbf{0}$), see Figure 1 and Eqs (B.2)–(B.3). The incident electric field from the left is

$$\boldsymbol{E}^i_{\text{left}}(t) = \boldsymbol{E}^i(t),$$

  and the reflected and transmitted electric fields are denoted by $\boldsymbol{E}^r(t)$ and $\boldsymbol{E}^t(t)$, respectively. The scattering geometry is depicted in Figure 4.

The solution of this problem can be obtained by linear superposition of the solutions of the following two wave-propagation problems:

- **Subproblem 1.** Find the solution $\boldsymbol{E}^{\pm}(z,t) = \boldsymbol{E}^{\pm}_1(z,t)$ of the dynamical equation (B.1) subject to the boundary conditions

$$\begin{cases} \boldsymbol{E}^i_1(t) = \dfrac{1}{1+r_0}\big(\boldsymbol{E}^+(+0,t) + r_0\boldsymbol{E}^-(+0,t)\big), \\ \boldsymbol{E}^-(d-0,t) = \mathbf{0}. \end{cases}$$

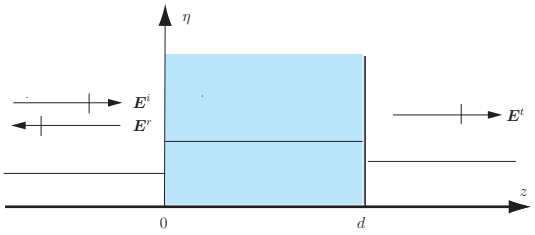

Figure 4: The optical impedance profile in the original scattering problem. $\boldsymbol{E}^i_{\text{left}}(t) = \boldsymbol{E}^i(t)$ and $\boldsymbol{E}^i_{\text{right}}(t) = \boldsymbol{0}$.

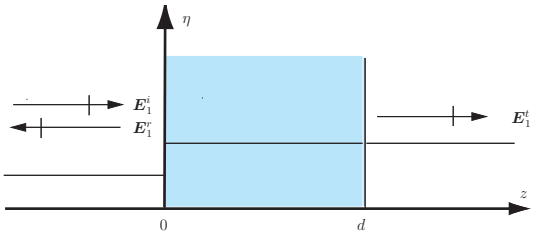

Figure 5: The optical impedance profile in subproblem 1. The incident electric field is $\boldsymbol{E}^i_1(t) = \boldsymbol{E}^i(t)$.

This is the partial mismatch-case $r_1 = 0$, $r_0 \neq 0$ obtained by setting $\eta(d+0) := \eta(d-0)$. The incident electric field is the same as in the original problem:

$$\boldsymbol{E}^i_{\text{left}}(t) = \boldsymbol{E}^i_1(t) = \boldsymbol{E}^i(t). \tag{B.5}$$

The reflected and transmitted electric fields in this problem are denoted by $\boldsymbol{E}^r_1(t)$ and $\boldsymbol{E}^t_1(t)$, respectively. The scattering geometry is depicted in Figure 5.

- **Subproblem 2.** Find the solution $\boldsymbol{E}^{\pm}(z,t) = \boldsymbol{E}^{\pm}_2(z,t)$ of the dynamical equation (B.1) subject to the boundary conditions

$$\begin{cases} \boldsymbol{E}^+(+0,t) = -r_0 \boldsymbol{E}^-(+0,t), \\ \boldsymbol{E}^i_2(t) = \dfrac{1}{1+r_1}\big(r_1 \boldsymbol{E}^+(d-0,t) + \boldsymbol{E}^-(d-0,t)\big), \end{cases}$$

where the incident electric field from the right is

$$\boldsymbol{E}^i_{\text{right}}(t) = \boldsymbol{E}^i_2(t) = -\frac{r_1}{1+r_1}\boldsymbol{E}^+_1(d-0,t) = -\frac{r_1}{1+r_1}\boldsymbol{E}^t_1(t). \tag{B.6}$$

The transmitted field $\boldsymbol{E}^t_1(t)$ is of course obtained from subproblem 1. This is the full mismatch case. However, the slab is now excited from the right and not from the left. The reflected electric field (at $z = d+0$) and transmitted electric field (at $z = -0$) are denoted by $\boldsymbol{E}^r_2(t)$ and $\boldsymbol{E}^t_2(t)$, respectively. The scattering geometry is depicted in Figure 6.

Alternatively, the solution of the original problem can be obtained by superposition of the solutions of the following two wave-propagation problems:

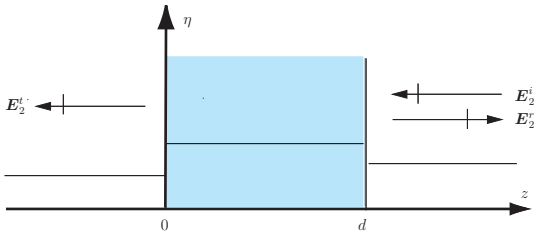

Figure 6: The optical impedance profile in subproblem 2. The incident electric field is $\boldsymbol{E}_2^i(t) = -r_1/(1+r_1)\boldsymbol{E}_1^t(t)$, where $\boldsymbol{E}_1^t(t)$ is the transmitted electric field in subproblem 1.

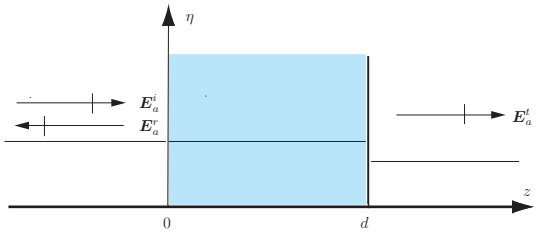

Figure 7: The optical impedance profile in subproblem a. The incident electric field is $\boldsymbol{E}_a^i(t) = (1+r_0)\boldsymbol{E}^i(t)$.

- **Subproblem a.** Find the solution $\boldsymbol{E}^{\pm}(z,t) = \boldsymbol{E}_4^{\pm}(z,t)$ of the dynamical equation (B.1) subject to the boundary conditions

$$\begin{cases} \boldsymbol{E}_a^i(t) = \boldsymbol{E}^+(+0,t), \\ \boldsymbol{E}^-(d-0,t) = -r_1\boldsymbol{E}^-(d-0,t). \end{cases}$$

  This is the partial mismatch-case $r_0 = 0$, $r_1 \neq 0$ obtained by setting $\eta(-0) := \eta(+0)$. The incident electric field from the left is

$$\boldsymbol{E}_{\text{left}}^i(t) = \boldsymbol{E}_a^i(t) = (1+r_0)\boldsymbol{E}^i(t). \tag{B.7}$$

  Recall that $\boldsymbol{E}^i(t)$ is the incident electric field of the original problem. The reflected and transmitted electric fields in this problem are denoted by $\boldsymbol{E}_a^r(t)$ and $\boldsymbol{E}_a^t(t)$, respectively. The scattering geometry is depicted in Figure 7.

- **Subproblem b.** Find the solution $\boldsymbol{E}^{\pm}(z,t) = \boldsymbol{E}_b^{\pm}(z,t)$ of the original problem, when the incident electric field from the left is

$$\boldsymbol{E}_{\text{left}}^i(t) = \boldsymbol{E}_b^i(t) = -\frac{r_0}{1+r_0}\boldsymbol{E}_a^-(+0,t) = -\frac{r_0}{1+r_0}\boldsymbol{E}_a^r(t). \tag{B.8}$$

  The electric field $\boldsymbol{E}_a^r(t)$ is obtained from subproblem a. The reflected and transmitted electric fields are denoted by $\boldsymbol{E}_b^r(t)$ and $\boldsymbol{E}_b^t(t)$, respectively. The scattering geometry is depicted in Figure 8.

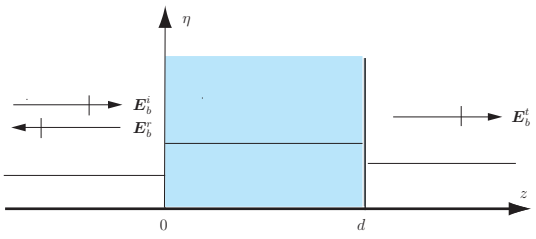

Figure 8: The optical impedance profile in subproblem b. The incident electric field is $\boldsymbol{E}_b^i(t) = -r_0/(1+r_0)\boldsymbol{E}_a^r(t)$,where $\boldsymbol{E}_a^r(t)$ is the reflected electric field in subproblem a.

By the first decomposition (subproblems 1–2), the discontinuity of the optical intrinsic impedance at the rear wall is removed at the cost of introducing scattering operators from the right. The second decomposition (subproblems a–b) eliminates the influence of the jump in the optical intrinsic impedance at the front wall. Incidence from the right need not be considered in this case.

B.3 Relations between scattering operators

The decomposition of the original problem into subproblem 1 and subproblem 2 is discussed first. The continuity of the total electric field at the back wall $z = d$ yields the result

$$\boldsymbol{E}^t(t) = \boldsymbol{E}_1^t(t) + \boldsymbol{E}_2^i(t) + \boldsymbol{E}_2^r(t). \tag{B.9}$$

In the same manner one obtains the relation

$$\boldsymbol{E}^r(t) = \boldsymbol{E}_1^r(t) + \boldsymbol{E}_2^t(t) \tag{B.10}$$

at the front wall $z = 0$.

The transmission and reflection operators of subproblem 1 are obtained from the scattering relation (B.4) by setting $r_1 = 0$:

$$\begin{cases} \mathcal{T}_{\text{left}}^{\text{right-match}} = (1+r_0)\mathbf{Q}^+\big(\mathbf{I} + \mathbf{T}_{\text{left}}^{\text{right-match}} *\big) \\ \mathcal{R}_{\text{left}}^{\text{right-match}} = r_0\mathbf{I} + (1-r_0^2)\mathbf{R}_{\text{left}}^{\text{right-match}} * \end{cases}$$

In terms of these operators, the identities

$$\begin{cases} \boldsymbol{E}^t = \mathcal{T}_{\text{left}}\delta_{\frac{d}{c}} * \boldsymbol{E}^i, \\ \boldsymbol{E}^r = \mathcal{R}_{\text{left}}\boldsymbol{E}^i, \end{cases} \quad \begin{cases} \boldsymbol{E}_1^t = \mathcal{T}_{\text{left}}^{\text{right-match}}\delta_{\frac{d}{c}} * \boldsymbol{E}_1^i, \\ \boldsymbol{E}_1^r = \mathcal{R}_{\text{left}}^{\text{right-match}}\boldsymbol{E}_1^i, \end{cases} \quad \begin{cases} \boldsymbol{E}_2^t = \mathcal{T}_{\text{right}}\delta_{\frac{d}{c}} * \boldsymbol{E}_2^i, \\ \boldsymbol{E}_2^r = \mathcal{R}_{\text{right}}\boldsymbol{E}_2^i \end{cases}$$

hold. Since all fields can be expressed in the electric field $\boldsymbol{E}_1^i(t)$ through the relations (B.5)–(B.6), straightforward insertion in equations (B.9)–(B.10) yields the operator identities

$$\begin{cases} \mathcal{T}_{\text{left}} = \dfrac{1}{1+r_1}\big(\mathcal{I} - r_1\mathcal{R}_{\text{right}}\big)\mathcal{T}_{\text{left}}^{\text{right-match}} \\ \mathcal{R}_{\text{left}} = \mathcal{R}_{\text{left}}^{\text{right-match}} - \dfrac{r_1}{1+r_1}\mathcal{T}_{\text{right}}\mathcal{T}_{\text{left}}^{\text{right-match}}\delta_{\frac{2d}{c}} * \end{cases} \tag{B.11}$$

In the special case, when the front wall is optically impedance-matched ($r_0 = 0$), equation (B.11) reduces to

$$\begin{cases} \mathcal{T}_{\text{left}}^{\text{left-match}} = \dfrac{1}{1+r_1}\big(\mathcal{I} - r_1\mathcal{R}_{\text{right}}^{\text{left-match}}\big)\mathcal{T}_{\text{left}}^{\text{match-match}} \\ \mathcal{R}_{\text{left}}^{\text{left-match}} = \mathcal{R}_{\text{left}}^{\text{match-match}} - \dfrac{r_1}{1+r_1}\mathcal{T}_{\text{right}}^{\text{left-match}}\mathcal{T}_{\text{left}}^{\text{match-match}}\delta_{\frac{2d}{c}}* \end{cases} \tag{B.12}$$

$$\begin{cases} \mathcal{T}_{\text{left}}^{\text{match-match}} = \mathbf{Q}^{+}\big(\mathbf{I} + \mathbf{T}_{\text{left}}^{\text{match-match}}\,*\,\big) \\ \mathcal{R}_{\text{left}}^{\text{match-match}} = \mathbf{R}_{\text{left}}^{\text{match-match}}* \end{cases}$$

are the scattering operators of the optically impedance-matched slab discussed in previous sections ($r_0 = r_1 = 0$) and

$$\begin{cases} \mathcal{T}_{\text{left}}^{\text{left-match}} = (1-r_1)\mathbf{Q}^{+}\big(\mathbf{I} + \mathbf{T}_{\text{left}}^{\text{left-match}}\,*\,\big) \\ \mathcal{R}_{\text{left}}^{\text{left-match}} = -r_1\mathbf{Q}^{+}\mathbf{Q}^{-}\delta_{\frac{2d}{c}}\,* + \mathbf{R}_{\text{left}}^{\text{left-match}}* \end{cases}$$

are the transmission and reflection operators of subproblem a ($r_0 = 0$).

For the decomposition of the original problem into subproblem a and subproblem b, the continuity of the total electric field yields the equation

$$\boldsymbol{E}^t(t) = \boldsymbol{E}_a^t(t) + \boldsymbol{E}_b^t(t)$$

at the back wall $z = d$, whereas the equality

$$\boldsymbol{E}^i(t) + \boldsymbol{E}^r(t) = \boldsymbol{E}_a^i(t) + \boldsymbol{E}_a^r(t) + \boldsymbol{E}_b^i(t) + \boldsymbol{E}_b^r(t)$$

holds at the front wall $z = 0$. Furthermore,

$$\begin{cases} \boldsymbol{E}^t = \mathcal{T}_{\text{left}}\delta_{\frac{d}{c}} * \boldsymbol{E}^i, \\ \boldsymbol{E}^r = \mathcal{R}_{\text{left}}\boldsymbol{E}^i, \end{cases} \quad \begin{cases} \boldsymbol{E}_a^t = \mathcal{T}_{\text{left}}^{\text{left-match}}\delta_{\frac{d}{c}} * \boldsymbol{E}_a^i, \\ \boldsymbol{E}_a^r = \mathcal{R}_{\text{left}}^{\text{left-match}}\boldsymbol{E}_a^i, \end{cases} \quad \begin{cases} \boldsymbol{E}_b^t = \mathcal{T}_{\text{left}}\delta_{\frac{d}{c}} * \boldsymbol{E}_b^i, \\ \boldsymbol{E}_b^r = \mathcal{R}_{\text{left}}\boldsymbol{E}_b^i. \end{cases}$$

Using the relations (B.7)–(B.8), all fields except the excitation $\boldsymbol{E}^i$ can be eliminated, and one obtains the operator equations (confer equations (A3) and (A2) of Ref. 8)

$$\begin{cases} \mathcal{T}_{\text{left}}\big(\mathcal{I} + r_0\mathcal{R}_{\text{left}}^{\text{left-match}}\big) = (1+r_0)\mathcal{T}_{\text{left}}^{\text{left-match}} \\ \big(\mathcal{I} + \mathcal{R}_{\text{left}}\big)\big(\mathcal{I} + r_0\mathcal{R}_{\text{left}}^{\text{left-match}}\big) = (1+r_0)\big(\mathcal{I} + \mathcal{R}_{\text{left}}^{\text{left-match}}\big). \end{cases} \tag{B.13}$$

In the special case, when the rear wall is optically impedance-matched ($r_1 = 0$), these equations reduce to

$$\begin{cases} \mathcal{T}_{\text{left}}^{\text{right-match}}\big(\mathcal{I} + r_0\mathcal{R}_{\text{left}}^{\text{match-match}}\big) = (1+r_0)\mathcal{T}_{\text{left}}^{\text{match-match}} \\ \big(\mathcal{I} + \mathcal{R}_{\text{left}}^{\text{right-match}}\big)\big(\mathcal{I} + r_0\mathcal{R}_{\text{left}}^{\text{match-match}}\big) = (1+r_0)\big(\mathcal{I} + \mathcal{R}_{\text{left}}^{\text{match-match}}\big). \end{cases} \tag{B.14}$$

To summarize, decomposition of the scattering problem (B.4) for the bi-isotropic slab subject to excitation from left only yields the operator equations (B.11)–(B.14). Another four operator equations are obtained by considering excitation from the

right only. These equations are most easily derived by making obvious substitutions in equations (B.11)–(B.14).

In particular, the equivalent of equation (B.14) is

$$\begin{cases} \mathcal{T}_{\text{right}}^{\text{left-match}}\big(\mathcal{I}+r_1\mathcal{R}_{\text{right}}^{\text{match-match}}\big)=(1+r_1)\mathcal{T}_{\text{right}}^{\text{match-match}} \\ \big(\mathcal{I}+\mathcal{R}_{\text{right}}^{\text{left-match}}\big)\big(\mathcal{I}+r_1\mathcal{R}_{\text{right}}^{\text{match-match}}\big)=(1+r_1)\big(\mathcal{I}+\mathcal{R}_{\text{right}}^{\text{match-match}}\big), \end{cases} \tag{B.15}$$

where

$$\begin{cases} \mathcal{T}_{\text{right}}^{\text{left-match}}=(1+r_1)\mathbf{Q}^-\big(\mathbf{I}+\mathbf{T}_{\text{right}}^{\text{left-match}}*\big) \\ \mathcal{R}_{\text{right}}^{\text{left-match}}=r_1\mathbf{I}+(1-r_1^2)\mathbf{R}_{\text{right}}^{\text{left-match}}* \end{cases}$$

and

$$\begin{cases} \mathcal{T}_{\text{right}}^{\text{match-match}}=\mathbf{Q}^-\big(\mathbf{I}+\mathbf{T}_{\text{right}}^{\text{match-match}}*\big) \\ \mathcal{R}_{\text{right}}^{\text{match-match}}=\mathbf{R}_{\text{right}}^{\text{match-match}}* \end{cases}$$

By substituting this result into equation (B.12), one obtains the useful relations

$$\mathcal{T}_{\text{left}}^{\text{left-match}}\big(\mathcal{I}+r_1\mathcal{R}_{\text{right}}^{\text{match-match}}\big)=(1-r_1)\mathcal{T}_{\text{left}}^{\text{match-match}} \tag{B.16}$$

and

$$\begin{gathered} \big(\mathcal{R}_{\text{left}}^{\text{left-match}}-\mathcal{R}_{\text{left}}^{\text{match-match}}\big)\big(\mathcal{I}+r_1\mathcal{R}_{\text{right}}^{\text{match-match}}\big)= \\ =-r_1\mathcal{T}_{\text{left}}^{\text{match-match}}\mathcal{T}_{\text{right}}^{\text{match-match}}\delta_{\frac{2d}{c}}* \end{gathered} \tag{B.17}$$

Finally, combination of equations (B.16)–(B.17) yields the equality

$$\begin{gathered} (1-r_1)^2\big(\mathcal{R}_{\text{left}}^{\text{left-match}}-\mathcal{R}_{\text{left}}^{\text{match-match}}\big)= \\ =-r_1\big(\mathcal{I}+r_1\mathcal{R}_{\text{left}}^{\text{match-match}}\big)\mathcal{T}_{\text{left}}^{\text{left-match}}(\mathcal{T}_{\text{left}}^{\text{left-match}})^t\delta_{\frac{2d}{c}}* \end{gathered} \tag{B.18}$$

Here, the relations

$$\begin{cases} (\mathcal{T}_{\text{right}}^{\text{match-match}})^t=\mathcal{T}_{\text{left}}^{\text{match-match}} \\ (\mathcal{R}_{\text{right}}^{\text{match-match}})^t=\mathcal{R}_{\text{left}}^{\text{match-match}} \end{cases}$$

have been employed.

The scattering relations (B.13) and (B.16)–(B.18) are referred to below.

B.4 Integral equations for the inverse problem

Straightforward analysis shows that the operator equations (B.13) can be written in the form (confer the integral equations on page 369 of Ref. 8)

$$\begin{cases} \mathbf{T}_{\text{left}}^{\text{left-match}}=\big(\mathbf{I}-r_0r_1\mathbf{Q}^+\mathbf{Q}^-\delta_{\frac{2d}{c}}*\big)\mathbf{T}_{\text{left}}+\big(\mathbf{I}-r_0r_1\mathbf{Q}^+\mathbf{Q}^-\delta_{\frac{2d}{c}}*\big)^{-1}r_0\mathbf{R}_{\text{left}}^{\text{left-match}}+ \\ \qquad\qquad +r_0\mathbf{T}_{\text{left}}*\mathbf{R}_{\text{left}}^{\text{left-match}} \\ \mathbf{R}_{\text{left}}^{\text{left-match}}=r_0(1-r_0)\mathbf{R}_{\text{left}}*\mathbf{R}_{\text{left}}^{\text{left-match}}+(1-r_0)\big(\mathbf{I}-r_0r_1\mathbf{Q}^+\mathbf{Q}^-\delta_{\frac{2d}{c}}*\big)\mathbf{R}_{\text{left}}+ \\ \qquad\qquad +\big(\mathbf{I}-r_0r_1\mathbf{Q}^+\mathbf{Q}^-\delta_{\frac{2d}{c}}*\big)^{-1}\big(\mathbf{I}-r_1\mathbf{Q}^+\mathbf{Q}^-\delta_{\frac{2d}{c}}*\big)r_0\mathbf{R}_{\text{left}}^{\text{left-match}} \end{cases}$$

These equations are seen to be equivalent to the integral equations

$$\begin{aligned}\mathbf{T}_{\text{left}}(t) - \mathbf{T}_{\text{left}}^{\text{left-match}}(t) + r_0\mathbf{R}_{\text{left}}^{\text{left-match}}(t) + r_0\big(\mathbf{T}_{\text{left}} * \mathbf{R}_{\text{left}}^{\text{left-match}}\big)(t) = \\ = r_0 r_1 \mathbf{Q}^+\mathbf{Q}^-\big(2\mathbf{T}_{\text{left}} - \mathbf{T}_{\text{left}}^{\text{left-match}} + r_0\mathbf{T}_{\text{left}} * \mathbf{R}_{\text{left}}^{\text{left-match}}\big)(t-2d/c) + \\ - (r_0 r_1 \mathbf{Q}^+\mathbf{Q}^-)^2\mathbf{T}_{\text{left}}(t-4d/c)\end{aligned} \tag{B.19}$$

and

$$\begin{aligned}\mathbf{R}_{\text{left}}(t) - \mathbf{R}_{\text{left}}^{\text{left-match}}(t) + r_0\big(\mathbf{R}_{\text{left}} * \mathbf{R}_{\text{left}}^{\text{left-match}}\big)(t) = \\ = r_0 r_1 \mathbf{Q}^+\mathbf{Q}^-\big(2\mathbf{R}_{\text{left}} + r_0\mathbf{R}_{\text{left}} * \mathbf{R}_{\text{left}}^{\text{left-match}}\big)(t-2d/c) + \\ - (r_0 r_1 \mathbf{Q}^+\mathbf{Q}^-)^2\mathbf{R}_{\text{left}}(t-4d/c),\end{aligned} \tag{B.20}$$

which hold for all times t. Similarly, equations (B.16) and (B.18) are equivalent to the integral equations

$$\begin{aligned}\mathbf{T}_{\text{left}}^{\text{match-match}}(t) = \mathbf{T}_{\text{left}}^{\text{left-match}}(t) + r_1\mathbf{R}_{\text{right}}^{\text{match-match}}(t) + \\ + r_1\big(\mathbf{T}_{\text{left}}^{\text{left-match}} * \mathbf{R}_{\text{right}}^{\text{match-match}}\big)(t)\end{aligned} \tag{B.21}$$

(confer equation (B1) of Ref. 8) and

$$\begin{aligned}\mathbf{R}_{\text{left}}^{\text{match-match}}(t) = \mathbf{R}_{\text{left}}^{\text{left-match}}(t) + \\ + r_1\mathbf{Q}^+\mathbf{Q}^- \times \big(\mathbf{C} + r_1\mathbf{R}_{\text{left}}^{\text{match-match}} + r_1\mathbf{R}_{\text{left}}^{\text{match-match}} * \mathbf{C}\big)(t-2d/c),\end{aligned} \tag{B.22}$$

respectively, where the matrix-kernel $\mathbf{C}(t)$ is

$$\mathbf{C}(t) = \mathbf{T}_{\text{left}}^{\text{left-match}}(t) + (\mathbf{T}_{\text{left}}^{\text{left-match}})^t(t) + \big(\mathbf{T}_{\text{left}}^{\text{left-match}} * (\mathbf{T}_{\text{left}}^{\text{left-match}})^t\big)(t).$$

The inverse scattering problem in the general mismatch case is now briefly discussed. The wave-front propagators $\mathbf{Q}^{\pm}$ and the optical reflection coefficients r_0 and r_1 of the slab are assumed to be known. The physical scattering kernels $\mathbf{T}_{\text{left}}(t)$ and $\mathbf{R}_{\text{left}}(t)$ constitute data.

First, the reflection kernel $\mathbf{R}_{\text{left}}^{\text{left-match}}(t)$ is obtained by solving the time-delayed Volterra equation of the second kind (B.20). This is a well posed problem [10]. Once this kernel is known, the transmission kernel $\mathbf{T}_{\text{left}}^{\text{left-match}}(t)$ is obtained from equation (B.19) by direct computation (convolution and addition) roundtrip by roundtrip. Similarly, the reflection kernel $\mathbf{R}_{\text{left}}^{\text{match-match}}(t)$ of the optically impedance-matched medium is obtained from equation (B.22). Finally, equation (B.21) yields the transmission kernel $\mathbf{T}_{\text{left}}^{\text{match-match}}(t)$ by direct computation. Knowing the kernels $\mathbf{R}_{\text{left}}^{\text{match-match}}(t)$, $\mathbf{T}_{\text{left}}^{\text{match-match}}(t)$ and the wave-front propagators $\mathbf{Q}^{\pm}$, the inverse algorithm presented in the previous sections can be employed.

B.5 Integral equations for the direct problem

In this subsection, the direct scattering problem is discussed. In the first step, the reflection kernel $\mathbf{R}_{\text{left}}^{\text{match-match}}(t)$ and the transmission kernel $\mathbf{T}_{\text{left}}^{\text{match-match}}(t)$ of the optically impedance-matched slab are obtained by employing a direct algorithm based on, e.g., the imbedding approach [15], the Green functions technique [15],

or the method with wave propagators and single-interface scattering operators [16]. The aim is compute the physical scattering kernels $\mathbf{R}_{\text{left}}(t)$ and $\mathbf{T}_{\text{left}}(t)$.

The operator equations (B.17) is easily seen to be equivalent to the integral equation (confer equation (B5) of Ref. 8)

$$\begin{aligned}\mathbf{R}_{\text{left}}^{\text{left-match}}(t) - \mathbf{R}_{\text{left}}^{\text{match-match}}(t) + \\ + r_1\Big(\mathbf{R}_{\text{right}}^{\text{match-match}} * \big(\mathbf{R}_{\text{left}}^{\text{left-match}} - \mathbf{R}_{\text{left}}^{\text{match-match}}\big)\Big)(t) = \\ = -r_1\mathbf{Q}^{+}\mathbf{Q}^{-}\mathbf{B}(t-2d/c),\end{aligned} \tag{B.23}$$

where the matrix-kernel $\mathbf{B}(t)$ evaluated at time t is

$$\begin{aligned}\mathbf{B}(t) = -r_1\mathbf{R}_{\text{right}}^{\text{match-match}}(t) + \mathbf{T}_{\text{left}}^{\text{match-match}}(t) + \mathbf{T}_{\text{right}}^{\text{match-match}}(t) + \\ + \big(\mathbf{T}_{\text{left}}^{\text{match-match}} * \mathbf{T}_{\text{right}}^{\text{match-match}}\big)(t).\end{aligned}$$

This is a Volterra integral equation of the second kind in the difference kernel $\mathbf{R}_{\text{left}}^{\text{left-match}}(t) - \mathbf{R}_{\text{left}}^{\text{match-match}}(t)$; therefore, the reflection kernel $\mathbf{R}_{\text{left}}^{\text{left-match}}(t)$ is uniquely determined by equation (B.23). Similarly, the transmission kernel $\mathbf{T}_{\text{left}}^{\text{left-match}}(t)$ is obtained by solving the Volterra integral equation of the second kind (B.21). The physical reflection kernel $\mathbf{R}_{\text{left}}(t)$ is obtained by solving the time-delayed Volterra integral equation of the second kind (B.20). Finally, by solving the time-delayed Volterra integral equation of the second kind (B.19), the physical reflection kernel $\mathbf{T}_{\text{left}}(t)$ is computed.

B.6 Alternative approach for free-space measurements

In this section, an alternative approach to the inverse scattering problem is discussed. The method is adjusted to a free-space measurement, that is, it is required that

$$r_0 = r_1.$$

This is an important special case. As an immediate consequence, scattering data fulfills

$$\begin{cases}\mathbf{T}_{\text{right}}(t) = \mathbf{T}_{\text{left}}^{t}(t), \\ \mathbf{R}_{\text{right}}(t) = \mathbf{R}_{\text{left}}^{t}(t).\end{cases}$$

The operator equation (B.11) is readily seen to be equivalent to the integral equations

$$\begin{aligned}\mathbf{T}_{\text{left}}(t) - \mathbf{T}_{\text{left}}^{\text{right-match}}(t) + r_1\mathbf{R}_{\text{right}}(t) + r_1\mathbf{T}_{\text{left}}^{\text{right-match}} * \mathbf{R}_{\text{right}}\big)(t) = \\ = r_0 r_1\mathbf{Q}^{+}\mathbf{Q}^{-}\big(\mathbf{T}_{\text{left}} + r_1\mathbf{R}_{\text{right}} + r_1\mathbf{T}_{\text{left}}^{\text{right-match}} * \mathbf{R}_{\text{right}}\big)(t-2d/c)\end{aligned} \tag{B.24}$$

and

$$\begin{aligned}\mathbf{R}_{\text{left}}(t) - \mathbf{R}_{\text{left}}^{\text{right-match}}(t) = r_1\mathbf{Q}^{+}\mathbf{Q}^{-}\mathbf{A}(t-2d/c) + \\ + r_0(r_1\mathbf{Q}^{+}\mathbf{Q}^{-})^2\big(\mathbf{T}_{\text{right}} + \mathbf{T}_{\text{right}} * \mathbf{T}_{\text{left}}^{\text{right-match}}\big)(t-4d/c),\end{aligned} \tag{B.25}$$

where the function $\mathbf{A}(t)$ evaluated at time t is

$$\mathbf{A}(t) = r_0\mathbf{R}_{\text{left}}(t) - r_0\mathbf{R}_{\text{left}}^{\text{right-match}}(t) - \mathbf{T}_{\text{right}}(t) - \mathbf{T}_{\text{left}}^{\text{right-match}}(t) + \\ - \big(\mathbf{T}_{\text{right}} * \mathbf{T}_{\text{left}}^{\text{right-match}}\big)(t).$$

Roundtrip for roundtrip, the transmission kernel $\mathbf{T}_{\text{left}}^{\text{right-match}}(t)$ is obtained by solving the Volterra equation of the second kind (B.24), while the reflection kernel $\mathbf{R}_{\text{left}}^{\text{right-match}}(t)$ is computed directly by employing equation (B.25). These are the scattering kernels for the slab with optically impedance-matched rear wall ($r_1 = 0$).

On the other hand, equations (B.19)–(B.20) reduce to

$$\begin{cases} \mathbf{T}_{\text{left}}^{\text{right-match}} + r_0\mathbf{R}_{\text{left}}^{\text{match-match}} + r_0\mathbf{T}_{\text{left}}^{\text{right-match}} * \mathbf{R}_{\text{left}}^{\text{match-match}} = \mathbf{T}_{\text{left}}^{\text{match-match}} \\ \mathbf{R}_{\text{left}}^{\text{right-match}} + r_0\mathbf{R}_{\text{left}}^{\text{right-match}} * \mathbf{R}_{\text{left}}^{\text{match-match}} = \mathbf{R}_{\text{left}}^{\text{match-match}} \end{cases} \tag{B.26}$$

The second identity is a Volterra equation of the second kind in the reflection kernel $\mathbf{R}_{\text{left}}^{\text{match-match}}(t)$, and, therefore, this kernel is uniquely determined. The first equality (B.26) yields the transmission kernel $\mathbf{T}_{\text{left}}^{\text{match-match}}(t)$. Finally, an inverse algorithm for the optically impedance-matched slab is applied to obtain the susceptibility kernels of the bi-isotropic medium.

In the direct problem, the scattering kernels $\mathbf{T}_{\text{left}}^{\text{right-match}}(t)$ and $\mathbf{R}_{\text{left}}^{\text{right-match}}(t)$ are computed first by solving the Volterra equations of the second kind (B.26). Then, the physical scattering kernels $\mathbf{T}_{\text{left}}(t)$ and $\mathbf{R}_{\text{left}}(t)$ are obtained from equations (B.24)–(B.25) by direct computation.

Appendix Acknowledgment

The work reported in this paper is supported by a grant from the Swedish Research Council for Engineering Sciences, and its support is gratefully acknowledged.

References

[1] D.F. Arago. Sur une modification remarquable qu'éprouvent les rayons lumineux dans leur passage à travers certains corps diaphanes, et sur quelques autres nouveaux phénomènes d'optique. *Mem. Inst.*, **1**, 93–134, 1811.

[2] J.B. Biot. Mémoire sur un nouveau genre d'oscillations que les molécules de la lumière éprouvent en traversant certains cristaux. *Mem. Inst.*, **1**, 1, 1812.

[3] J.H. Cloete and A.G. Smith. The constitutive parameters of a lossy chiral slab by inversion of plane-wave scattering coefficients. *Microwave and Optical Technology Letters*, **5**, 303–306, 1992. Correction: Vol., No.1, 1994.

[4] N. Engheta and D.L. Jaggard. Electromagnetic chirality and its applications. *IEEE Antennas and Propagation Society Newsletter*, pages 6–12, October 1988.

[5] A. Fresnel. Mémoire sur la double réfraction que les rayons lumineux éprouvent en traversant les aiguilles de cristal de roche suivant des directions paralleles a l'axe. *Oeuvres*, **1**, 731–751, 1822.

[6] J.D. Jackson. *Classical Electrodynamics*. John Wiley & Sons, New York, second edition, 1975.

[7] A. Karlsson and G. Kristensson. Constitutive relations, dissipation and reciprocity for the Maxwell equations in the time domain. *J. Electro. Waves Applic.*, **6**(5/6), 537–551, 1992.

[8] G. Kristensson and R.J. Krueger. Direct and inverse scattering in the time domain for a dissipative wave equation. Part 3: Scattering operators in the presence of a phase velocity mismatch. *J. Math. Phys.*, **28**(2), 360–370, 1987.

[9] G. Kristensson and S. Rikte. The inverse scattering problem for a homogeneous bi-isotropic slab using transient data. In L. Päivärinta and E. Somersalo, editors, *Inverse Problems in Mathematical Physics*, pages 112–125. Springer, Berlin, 1993.

[10] R.J. Krueger. Some Results on Linear Delay Integral Equations. *Journal of Mathematical Analysis and Applications*, **67**(1), 233–238, 1979.

[11] A. Lakhtakia. Recent contributions to classical electromagnetic theory of chiral media: what next? *Speculations in Science and Technology*, **14**(1), 2–17, 1991.

[12] I.V. Lindell, A.H. Sihvola, S.A. Tretyakov, and A.J. Viitanen. *Electromagnetic Waves in Chiral and Bi-isotropic Media*. Artech House, Boston-London, 1994.

[13] K.F. Lindman. Om en genom ett isotropt system av spiralformiga resonatorer alstrad rotationspolarisation av de elektromagnetiska vågorna. *Översigt af Finska Vetenskaps-Societetens förhandlingar, A. Matematik och naturvetenskaper*, **LVII**(3), 1–32, 1914–1915.

[14] R. Redheffer. On the relation of transmission-line theory on scattering and transfer. *J. Math. Phys.*, **41**, 1–41, 1962.

[15] S. Rikte. Reconstruction of bi-isotropic material parameters using transient electromagnetic fields. Technical Report LUTEDX/(TEAT-7033)/1–22/(1994), Lund Institute of Technology, Department of Electromagnetic Theory, P.O. Box 118, S-211 00 Lund, Sweden, 1994.

[16] S. Rikte. The Theory of the Propagation of TEM-Pulses in Dispersive Bi-isotropic Slabs. Technical Report LUTEDX/(TEAT-7040)/1–22/(1995), Lund Institute of Technology, Department of Electromagnetic Theory, P.O. Box 118, S-211 00 Lund, Sweden, 1995.

[17] S. Rikte. Existence, uniqueness, and causality theorems for wave propagation in stratified, temporally dispersive, complex media. *SIAM J. Math. Anal.*, 1997. (in press).